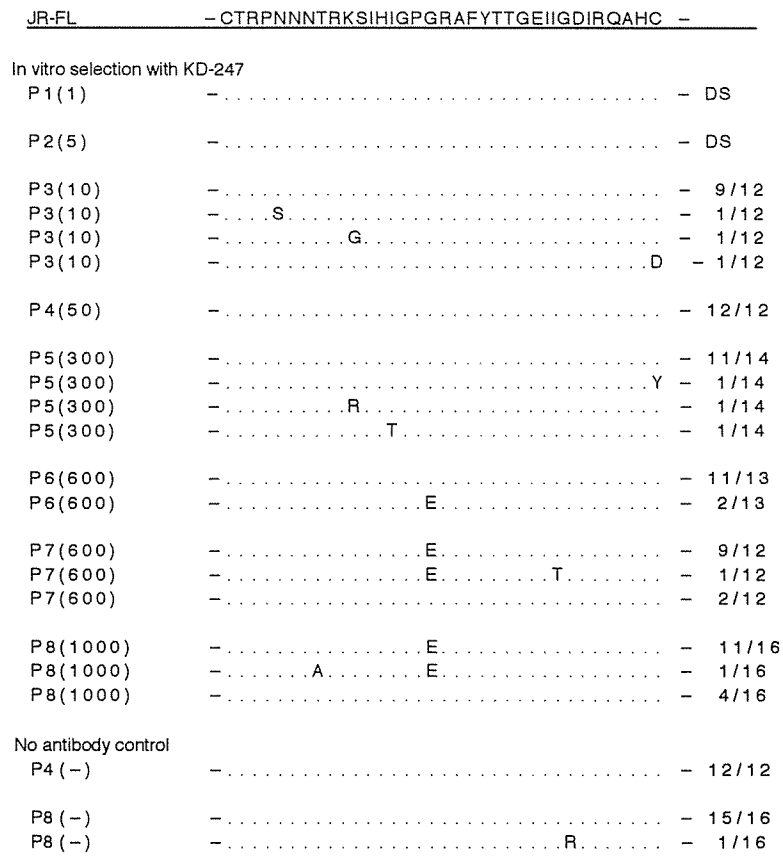

Fig. 1. V3 amino acid sequences from the supernatants of JR-FL-infected PM1/CCR5 cells passaged in the presence or absence of KD-247. Viral RNA from the cell culture supernatants at several concentrations of KD-247 was reverse-transcribed. After subjecting the obtained cDNA to PCR amplification and cloning, the *env* regions in the viruses passaged in the presence or absence of KD-247 were sequenced. The wild-type JR-FL amino acid sequence of V3 is shown at the top. The numbers on the right show the numbers of clones with the listed sequence among the total number of clones tested. In each set of clones, the deduced amino acid sequence of the V3 region was aligned by the single amino acid code. Dots denote sequence identity. DS, Direct sequence.

without KD-247 did not show the G314E substitution at either passage 4 (0/12 clones) or passage 8 (0/16 clones) (Fig. 1).

Susceptibilities of HIV-1 containing the KD-247-associated G314E substitution to MAb and drugs

To confirm whether the G314E mutation was responsible for the reduced sensitivity to KD-247, a single-round replication assay was performed. Luciferase-reporter viruses were pseudotyped with wild-type JR-FL (JR-FL_{wt}) or singly mutated with G314E (JR-FL_{G314E}) in the V3 region. As shown in Fig. 2a, JR-FL_{G314E} was completely resistant to KD-247 up to 100 μg/ml. We also examined the sensitivities of the pseudotyped clones to rsCD4, anti-CD4 MAb RPA-T4 and anti-CCR5 MAb 2D7 by a single-round replication assay (Fig. 2b–d). As expected, JR-FL_{G314E} was more sensitive to rsCD4 and 2D7, but fourfold more resistant to RPA-T4, compared to JR-FLwt, similar to the results for the passaged viruses with or without KD-247.

Next, we determined the sensitivities of JR-FL_{G314E} to three CCR5 inhibitors (TAK-779, SCH-C and AK-602). The IC_{50} values of TAK-779, SCH-C and AK-602 against JR-FL_{G314E} were 20-, 10- and 5-fold lower than the corresponding values against JR-FL_{wt}, respectively (Fig. 2e–g). These results confirmed that the G314E mutation was associated with the observed reduction in the sensitivities of JR-FL(1000)8P to KD-247 and RPA-T4, and also with the increased sensitivities to rsCD4, 2D7 and CCR5 inhibitors.

Next, we analysed the sensitivities of JR-FL_{wt} and JR-FL_{G314E} to another broad-specificity neutralizing anti-V3 MAb 447-52D and the CD4i MAb 17b (Fig. 2h and i). Interestingly, JR-FL_{G314E} was more sensitive to both 17b (< 0.8-fold change in the IC_{50}) and 447-52D (0.1-fold change in the IC_{50}) than JR-FLwt (Fig. 2h and i). A similar result regarding neutralization sensitivity to 17b was reported when viruses were pretreated with rsCD4 [16]. In our result, JR-FL_{G314E} was more sensitive to 17b

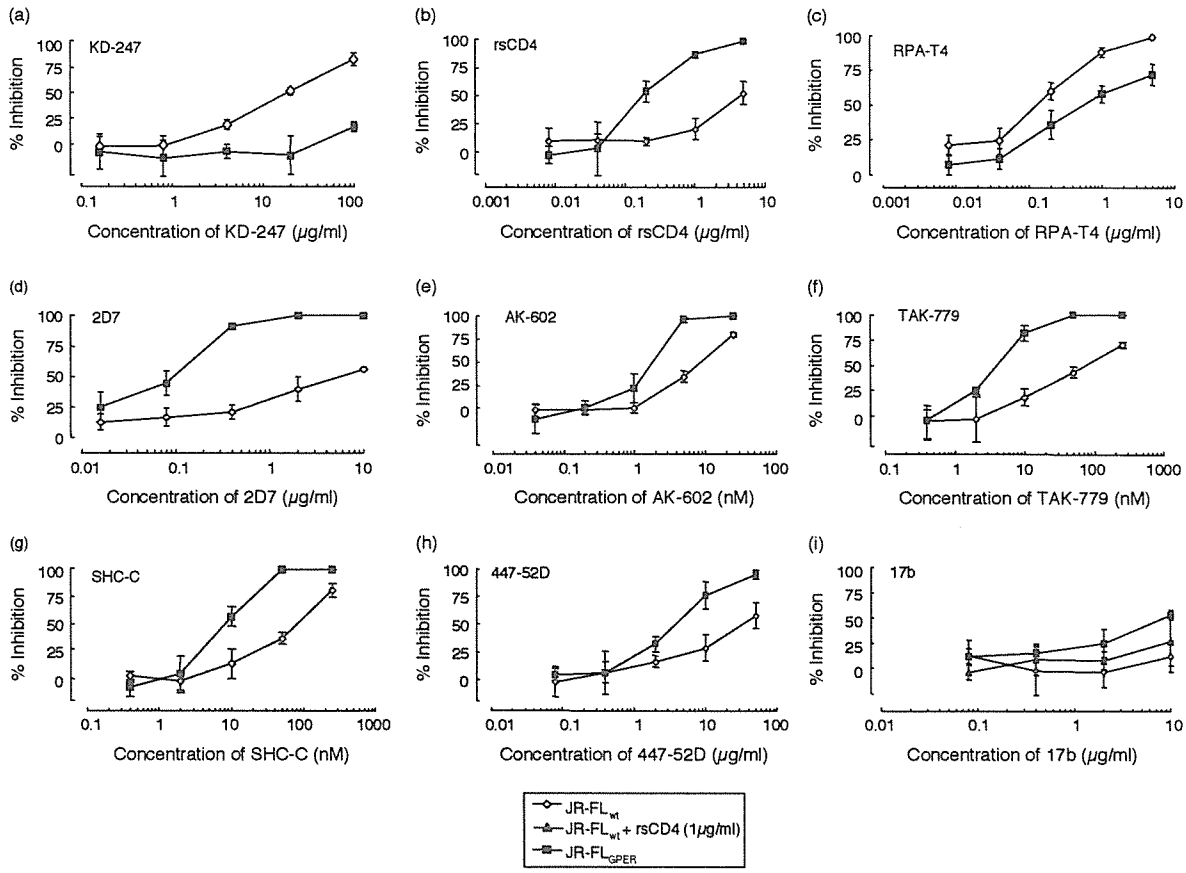

Fig. 2. Sensitivities of luciferase reporter HIV strains pseudotyped with the G314E envelope mutation to MAb, rsCD4 and CCR5 inhibitors. KD-247 (a), rsCD4 (b), 447-52D (h) and 17b with or without rsCD4 (1 μg/ml) (i) were preincubated with luciferase reporter HIVs pseudotyped with wild-type JR-FL (JR-FL_{wt}) or the G314E envelope mutant (JR-FL_{GPER}) for 15 min, followed by addition of the mixtures to the target cells (GOHST-hi5). The target cells were treated with RPA-T4 (c), 2D7 (d), AK-602 (e), TAK-779 (f) and SCH-C (g) for 15 min, followed by an inoculation of the pseudotype clones. Inhibitory effects were determined by measuring the luciferase activities on day 2 of culture.

than JR-FLwt preincubated with rsCD4 (1 μg/ml) (Fig. 2i).

Comparison of antibody binding to cell surface-expressed wild-type and GPER mutant Env

To elucidate the mechanism of the increased sensitivities of the escape virus with the G314E mutation in the V3-tip to 17b and 447-52D, wild-type or mutant Env-expressing 293T cells were established by transfecting each Env expression plasmid, and then stained with the MAb in the presence or absence of rsCD4 (0.5 μg/ml). Binding of a patient's IgG, KD-247, 17b or 447-52D to the surface-expressed Env proteins was assayed using a fluorescence-activated cell sorter analysis. As shown in Fig. 3, KD-247 bound to the wild-type JR-FL Env, but not the GPER mutant Env, while the other anti-V3 MAb, 447-52D, bound to both the Env proteins very well, especially the mutant Env. The mean fluorescence intensity (MFI) of 447-52D increased from 87.56 (wild-type Env) to 219.47 (GPER Env). Without rsCD4, the CD4i 17b MAb bound slightly to the wild-type Env (MFI, 33.21; Fig. 3) but failed to neutralize JR-FL_{wt} (Fig. 2i). On the other hand, in the presence of rsCD4 (0.5 μg/ml), a shift in the MFI was observed with 17b binding to the surface of wild type-Env-expressing cells. In contrast to these data for wild-type Env, 17b bound to the mutant Env efficiently in the absence of rsCD4 at a higher level than to the wild-type Env in the presence of rsCD4 (MFI, 97.33 for the mutant Env versus 56.61 for the wild-type Env; Fig. 3). 17b was also able to neutralize JR-FL_{GPER}, even in the absence of rsCD4 (Fig. 2i). These results suggest that the G314E mutation in the V3-tip induces the expression of cryptic epitopes for antibodies against the CD4i epitope and V3 loop, such that the mutant virus is neutralized by the CD4i MAb without rsCD4 or by lower concentrations of the anti-V3 MAb compared with the wild-type virus.

Highly synergistic interactions of KD-247 combined with CCR5 inhibitors

Both neutralizing MAb and chemokine receptor inhibitors attack the viral entry process, especially at the stage of the chemokine receptor-gp120 (V3)

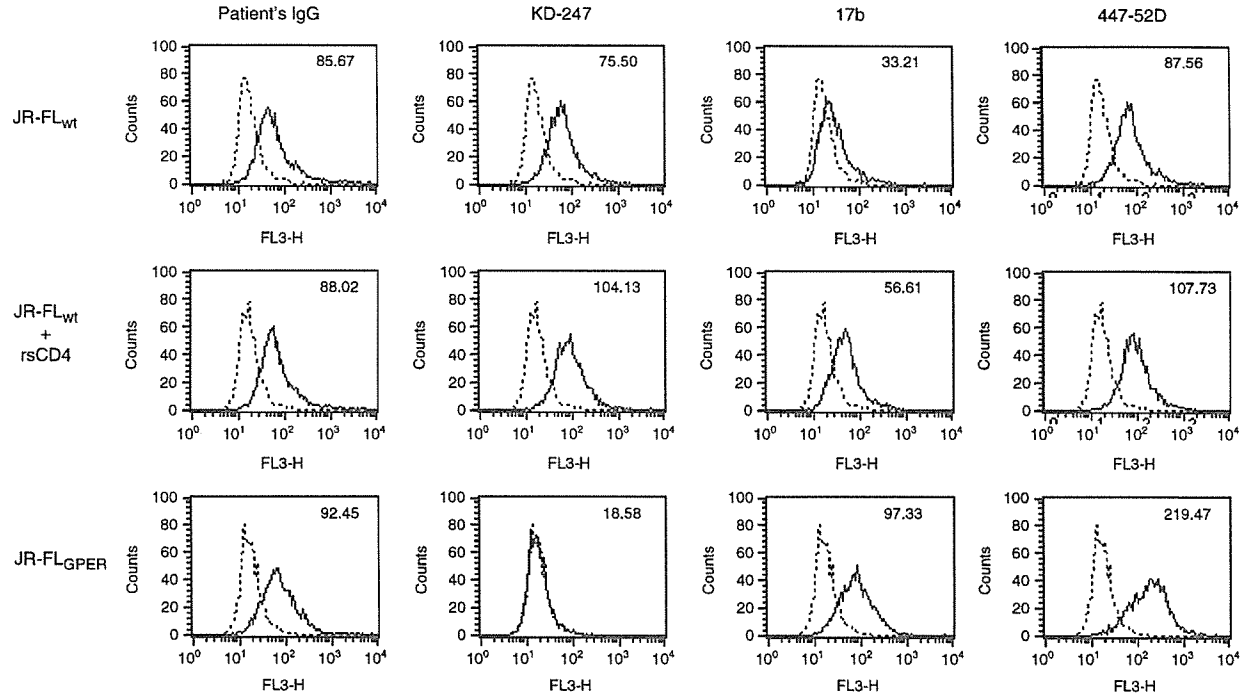

Fig. 3. Comparison of antibody binding to cell surface-expressed wild-type and GPER mutant Envs. 293T cells transfected with wild-type and GPER mutant Env-expression vectors were harvested at 36 h post-transfection and stained with the indicated antibodies. Flow cytometry data for binding of the indicated antibodies (black lines) to cell surface wild-type Env (upper), wild-type Env in the presence of 0.5 μg/ml of rsCD4 (middle) and GPER mutant Env (lower) are shown among GFP-gated 293T cells along with a control antibody (anti-human CD19; dotted lines). Data are representative of the results from at least two independent experiments. The number at the top right of each graph shows the MFI of the indicated antibodies.

interaction. Each of them binds to either CCR5 or gp120. Furthermore, our present observations suggest that the neutralizing MAb KD-247 selects an escape variant with greater sensitivity to chemokine receptor inhibitors. Based on this notion, we attempted to test the synergy of this MAb with chemokine receptor inhibitors against wild-type JR-FL.

The multiple-drug-effect analysis of Chou and colleagues [14,15] was used to analyse the effects of combinations of KD-247 with CCR5 inhibitors against JR-FL(−)8P in PM1/CCR5 cells (Table 2). As shown in Table 2, all the CI values for KD-247 with the CCR5 inhibitors (TAK-779, AK-602 or SCH-C) were < 0.5 against JR-FL(−)8P at all the inhibitory concentrations tested. In particular, the CI values for the combinations of KD-247 with SCH-C and AK-602 were less than 0.1 for IC_{90}. These results suggest that combination of KD-247 with any of the tested CCR5 inhibitors produces very highly synergistic interactions at not only high but also low inhibitory concentrations. We further evaluated the *in vitro* interactions between KD-247 and representatives of each class of currently available antiretroviral agents. Although KD-247 had favourable drug interactions with all of the agents (data not shown), the synergistic effects of KD-247 and CCR5 inhibitors were the most potent among all the combinations tested in this study.

Table 2. Combination indices (CI) for KD-247 and CCR5 inhibitors against virus JR-FL(−)8P.

CCR5 inhibitor used in combination with KD-247 (2.5–160 μg/ml)	CI values at different IC[a]		
	IC_{50}	IC_{75}	IC_{90}
AK-602 (0.3–20 nM)	0.21	0.12	0.07
TAK-779 (12.5–800 nM)	0.23	0.19	0.16
SCH-C (3–100 nM)	0.18	0.08	0.04

[a]The multiple-drug-effect analysis of Chou and colleagues was used to analyse the effects of the drugs in combination [15]. IC, Inhibitory concentration. CI < 1, synergy; 0.9 < CI < 1.1, additivity; CI > 1.1, antagonism.

Discussion

Although KD-247 shows clinical promise as a passive immunization agent for suppressing viral spread in phenotype-matched HIV-infected individuals, we also know that HIV-1 always escapes from the selection pressure of any one inhibitor by obtaining mutation(s). Therefore, we induced an HIV-1 variant that could escape from neutralization by KD-247 *in vitro* by continuously exposing the R5 virus JR-FL to increasing concentrations of KD-247 and defined the virological

properties and susceptibilities of this variant to other monoclonal antibodies (CD4i, anti-V3, anti-CD4 and anti-CCR5 MAb). The present data suggest that the KD-247 escape variant, which has a G314E mutation in the V3-tip, has not only a highly resistant phenotype against KD-247 but also greater sensitivities to CCR5 inhibitors and rsCD4, and needs higher concentration of anti-CD4 antibody for entry blocking compared with the corresponding control virus after eight passages in the absence of KD-247. These phenomena were confirmed using a pseudotyped virus containing the KD-247 escape-related G314E mutation by a single-round neutralizing assay. No previous studies have reported this G314E mutation in the V3-tip region of the R5 virus using in vitro selection by MAb. This mutation is also very rare in clinical isolates from HIV-1-infected patients [17]. Interestingly, this mutation in the V3-tip also influences the sensitivities to CCR5 inhibitors, rsCD4, anti-CD4 MAb and CD4i MAb 17b. It is not clear why KD-247 escape mutant became sensitive to rsCD4 and CCR5 inhibitors. It is conceivable that higher expression of CCR5 and CD4 on PM1/CCR5 cells may have some effect on the selection of such phenotype.

The ability to provide effective long-term antiretroviral therapy for HIV-1 infection has become a complex issue, since 40–50% of patients who initially achieve favourable viral suppression to undetectable levels subsequently experience treatment failure [18]. Moreover, a recent study reported that viruses with resistance to at least one drug were present in 1 of 10 antiretroviral-naive patients in Europe [19]. As more drug-resistant HIV-1 isolates emerge, new classes of potent antiretroviral agents targeting different steps of the HIV replicative cycle and new combinations of agents targeting different molecules, such as gp120 and CD4 or CCR5, are a welcome addition to the HIV arsenal. CCR5 inhibitors represent a new class of agents aimed at inhibiting viral entry. Following binding of gp120 to the CD4 receptor, CCR5 antagonists inhibit the interaction of gp120 with its coreceptor, an integral step in the fusion of HIV to the host cell [6–8]. As with other antiretroviral agents, resistance will likely prove to be a problem for CCR5 inhibitors [4,20]. Thus, the best strategy for preventing the occurrence of resistance is to use them in combination with other potent antiretroviral drugs. In the present study, we found that combinations of KD-247 with CCR5 inhibitors showed very strong synergistic interactions. When both antiviral reagents become available in the near future, these combinations will represent an efficient weapon against HIV-1. However, the benefit of these combinations to patients with HIV-1 infection needs to be further evaluated in clinical trials.

Taken together, the present data suggest that KD-247 has at least five advantages: (i) it exerts potent activity against a wide spectrum of subtype B HIV-1 variants, presumably due to its interaction with the IGPGR sequence in the gp120 V3 tip; (ii) viral acquisition of KD-247-resistance requires a very high concentration of KD-247 *in vitro*; (iii) at least some representatives of each class of currently available antiretroviral agents remain active against the virus variant selected *in vitro* with KD-247; (iv) the escape variant becomes more sensitive to CCR5 inhibitors and rsCD4, and is less dependent on CD4 binding for entry; and (v) combinations of KD-247 with CCR5 inhibitors show highly synergistic interactions at all inhibitory concentrations tested to date.

Acknowledgements

We thank J. Robinson for kindly providing the 17b, S. Zolla-Pazner for kindly providing the 447-52D, and Hirotomo Nakata, Kenji Maeda and Yasuhiro Kou for technical support. We also thank Yuki Azakami for excellent technical assistance.

This work was supported in part by the Ministry of Health, Labor and Welfare of Japan (H-16-AIDS-001 and -012), Grant-in-aid for Scientific Research (C-18591119) from the Ministry of Education, Science and Culture of Japan and the Cooperative Research Project on Clinical and Epidemiological Studies of Emerging and Re-emerging Infectious Diseases.

References

1. Eda Y, Takizawa M, Murakami T, Maeda H, Kimachi K, Yonemura H, *et al.* **Sequential immunization with V3 peptides from primary HIV-1 produces cross-neutralizing antibodies against primary isolates with matching narrow neutralization sequence motif.** *J Virol* 2006; **80**:5552–5562.
2. LaRosa GJ, Davide JP, Weinhold K, Waterbury JA, Profy AT, Lewis JA, *et al.* **Conserved sequence and structural elements in the HIV-1 principal neutralizing determinant.** *Science* 1990; **249**:932–935.
3. Eda Y, Murakami T, Ami Y, Nakasone T, Takizawa M, Someya K, *et al.* **Anti-V3 humanized antibody KD-247 effectively suppresses ex vivo generation of human immunodeficiency virus type 1 and affords sterile protection of monkeys against a heterologous simian/human immunodeficiency virus infection.** *J Virol* 2006; **80**:5563–5570.
4. Yusa K, Maeda Y, Fujioka A, Monde K, Harada S. **Isolation of TAK-779-resistant HIV-1 from an R5 HIV-1 GP120 V3 loop library.** *J Biol Chem* 2005; **280**:30083–30090.
5. Cecilia D, KewalRamani VN, O'Leary J, Volsky B, Nyambi P, Burda S, *et al.* **Neutralization profiles of primary human immunodeficiency virus type 1 isolates in the context of coreceptor usage.** *J Virol* 1998; **72**:6988–6996.
6. Baba M, Nishimura O, Kanzaki N, Okamoto M, Sawada H, Iizawa Y, *et al.* **A small-molecule, nonpeptide CCR5 antagonist with highly potent and selective anti-HIV-1 activity.** *Proc Natl Acad Sci USA* 1999; **96**:5698–5703.
7. Strizki JM, Xu S, Wagner NE, Wojcik L, Liu J, Hou Y, *et al.* **SCH-C (SCH 351125), an orally bioavailable, small molecule antagonist of the chemokine receptor CCR5, is a potent inhibitor of HIV-1 infection in vitro and in vivo.** *Proc Natl Acad Sci USA* 2001; **98**:12718–12723.
8. Maeda K, Nakata H, Koh Y, Miyakawa T, Ogata H, Takaoka Y, *et al.* **Spirodiketopiperazine-based CCR5 inhibitor which preserves CC-chemokine/CCR5 interactions and exerts potent activity against R5 human immunodeficiency virus type 1 in vitro.** *J Virol* 2004; **78**:8654–8662.

9. Maeda Y, Foda M, Matsushita S, Harada S. **Involvement of both the V2 and V3 regions of the CCR5-tropic human immunodeficiency virus type 1 envelope in reduced sensitivity to macrophage inflammatory protein 1alpha.** *J Virol* 2000; **74**: 1787–1793.
10. Yoshimura K, Feldman R, Kodama E, Kavlick F, Qiu YL, Zemlicka J, *et al.* **In vitro induction of human immunodeficiency virus type 1 variants resistant to phosphoralaninate prodrugs of Z-methylenecyclopropane nucleoside analogues.** *Antimicrob Agents Chemother* 1999; **43**:2479–2483.
11. Yoshimura K, Kato R, Kavlick MF, Nguyen A, Maroun V, Maeda K, *et al.* **A potent human immunodeficiency virus type 1 protease inhibitor, UIC-94003 (TMC-126), and selection of a novel (A28S) mutation in the protease active site.** *J Virol* 2002; **76**:1349–1358.
12. Hope TJ, Huang XJ, McDonald D, Parslow TG. **Steroid-receptor fusion of the human immunodeficiency virus type 1 Rev transactivator: mapping cryptic functions of the arginine-rich motif.** *Proc Natl Acad Sci USA* 1990; **87**:7787–7791.
13. Wang FX, Kimura T, Nishihara K, Yoshimura K, Koito A, Matsushita S. **Emergence of autologous neutralization-resistant variants from preexisting human immunodeficiency virus (HIV) quasi species during virus rebound in HIV type 1-infected patients undergoing highly active antiretroviral therapy.** *J Infect Dis* 2002; **185**:608–617.
14. Chou TC, Hayball MP. *CalcuSyn.* 2nd edn. Cambridge, UK: Biosoft; 1996.
15. Chou TC, Talaly P. **A simple generalized equation for the analysis of multiple inhibitions of Michaelis–Menten kinetic systems.** *J Biol Chem* 1977; **252**:6438–6442.
16. Decker JM, Bibollet-Ruche F, Wei X, Wang S, Levy DN, Wang W, *et al.* **Antigenic conservation and immunogenicity of the HIV coreceptor binding site.** *J Exp Med* 2005; **201**:1407–1419.
17. Kuiken C, Foly B, Hahn BH, Marx P, McCutchan F, Mellors J, *et al. HIV Sequence Compendium.* Los Alamos: Los Alamos National Laboratory; 2001.
18. Richman DD. **HIV chemotherapy.** *Nature* 2001; **410**:995–1001.
19. Wensing AM, van de Vijver DA, Angarano G, Asjo B, Ballota C, Boeri E, *et al.* **Prevalence of drug-resistant HIV-1 variants in untreated individuals in Europe: implications for clinical management.** *J Infect Dis* 2005; **192**:958–966.
20. Marozsan AJ, Kuhmann SE, Morgan T, Herrera C, Rivera-Troche E, Xu S, *et al.* **Generation and properties of a human immunodeficiency virus type 1 isolate resistant to the small molecule CCR5 inhibitor, SCH-417690 (SCH-D).** *Virology* 2005; **338**: 182–199.

DOI: 10.1002/cmdc.200600103

Bis-Tetrahydrofuran: a Privileged Ligand for Darunavir and a New Generation of HIV Protease Inhibitors That Combat Drug Resistance

Arun K. Ghosh,*[a] Perali Ramu Sridhar,[a] Nagaswamy Kumaragurubaran,[a] Yasuhiro Koh,[b] Irene T. Weber,[c] and Hiroaki Mitsuya[b, d]

Introduction

The acquired immunodeficiency syndrome (AIDS) epidemic continues to be a major challenge in medicine worldwide. According to the World Health Organization (WHO), the total number of people living with the human immunodeficiency virus (HIV) has reached an estimated 40.3 million, including nearly 5 million people newly infected with the virus in 2005.[1] The magnitude of the HIV/AIDS pandemic is truly astounding. Soon after the discovery of HIV as the etiological agent for AIDS, many biochemical targets were identified to combat this devastating disease.[2,3] During viral replication, *gag* and *gag-pol* gene products are translated as precursor polyproteins. These proteins are processed by a virally encoded protease to provide structural proteins (p17, p24, p9, and p7) and essential viral enzymes (including protease, reverse transcriptase, and integrase).[4] As a consequence, the retroviral enzymes reverse transcriptase (RT), integrase (IN), and protease (PR) were identified as potential drug targets. Therapeutic inhibition of the virally encoded HIV protease became particularly attractive because of prior knowledge of mechanism-based inhibition of other aspartyl proteases. In a combination therapy with a reverse transcriptase inhibitor, the protease inhibitor saquinavir (Invirase, **1**) discovered by researchers at Hoffman–LaRoche, was the first to receive approval by the United States Food and Drug Administration (FDA) in 1996 for the treatment of AIDS.[5,6] To date, a number of other protease inhibitors have been approved, and several others are undergoing advanced clinical trials. Combination therapy or highly active antiretroviral therapy (HAART), which uses HIV protease inhibitors and reverse transcriptase inhibitors, has become the major treatment regimen for AIDS.[7] Whereas HAART therapies have definitely improved the course of HIV management and halted the progression of AIDS, the majority of protease inhibitors contain substantial peptide-like features. As a result, anti-protease therapy suffers from the traditional problems of peptide-based drugs such as poor absorption, aqueous solubility, and metabolic instability. The most alarming is the rapid emergence of drug resistance, rendering these therapies ineffective.[8] Conceivably, new-generation nonpeptidal protease inhibitors that maintain potency against mutant strains resistant to the currently approved protease inhibitors may substantially delay the emergence of clinical resistance and may alleviate the problems of "peptide-based" drugs.[9] Thus, ready availability of a number of protein–ligand X-ray crystal structures and many elegant structure–activity studies have provided new opportunities and challenges for the structure-based design of protease inhibitors to combat drug resistance.[10,11]

Background

Human immunodeficiency virus (HIV) is a member of the lentivirus subfamily of retroviruses and, like other retroviruses, contains three major genes (*gag*, *pol*, and *env*).[12] The *pol* gene encodes for the enzymes reverse transcriptase (RT), integrase (IN), and protease (PR), which are critical for viral replication. Viral assembly begins with the association of the genomic RNA with the *gag* and *gag-pol* polyproteins, the primary translational products of the viral genome. The function of the protease is to cleave the polyproteins into functional proteins essential for the production of infectious progeny virus. The active form of the protease is a homodimeric endopeptidase of the aspartyl protease family.[13] Each monomer is made up of 99 amino acids, each contributing an aspartic acid residue to form the catalytic site.[13] Inactivation of the protease by either site-di-

[a] *Prof. A. K. Ghosh, Dr. P. Ramu Sridhar, Dr. N. Kumaragurubaran*
Departments of Chemistry and Medicinal Chemistry
Purdue University, West Lafayette, IN 47907 (USA)
Fax: (+1) 765-496-1612
E-mail: akghosh@purdue.edu

[b] *Dr. Y. Koh, Prof. H. Mitsuya*
Departments of Hematology and Infectious Diseases
Kumamoto University School of Medicine
Kumamoto 860-8556 (Japan)

[c] *Prof. I. T. Weber*
Department of Biology, Molecular Basis of Disease
Georgia State University, Atlanta, GA 30303 (USA)

[d] *Prof. H. Mitsuya*
Experimental Retrovirology Section
HIV and AIDS Malignancy Branch
National Cancer Institute, Bethesda, MD 20892 (USA)

rected mutagenesis or chemical inhibition leads to the production of immature, noninfectious viral particles, thus making the protease an attractive target for antiviral therapy.[14] Based on the transition-state mimetic concept that uses various nonhydrolyzable hydroxyethylene and hydroxyethylamine isosteres, an incredible effort has been carried out by academic and pharmaceutical research laboratories to design and develop potent protease inhibitors (PIs).[15] Early research involved the discovery of peptidomimetic inhibitors. More current emphasis has been to minimize molecular size, decrease peptide-like features, and design functionalities to combat drug resistance. Beside saquinavir (SQV, **1**),[5,6] seven other protease inhibitors have also been approved by the FDA for the treatment of AIDS in combination with reverse transcriptase inhibitors (Figure 1). These include: indinavir (IDV, **2**),[16] nelfinavir (NFV, **3**),[17] ritonavir (RTV, **4**),[18] atazanavir (ATV, **5**),[19] lopinavir (LPV, **6**),[20] amprenavir (APV, **7**),[21] and tipranavir (TPV, **8**).[22] Nelfinavir (**3**) and lopinavir (**6**) possess the same core unit as saquinavir (**1**) and ritonavir (**4**), respectively. However, the pharmacological properties and drug resistance profiles of **3** and **6** are very different from the corresponding inhibitors **1** and **4**.

In the clinical setting, all of these protease inhibitors have shown remarkable effectiveness.[23] As many as 90% of the clinical trial participants who received a protease inhibitor along with zidovudine (AZT) and lamivudine (3TC) have shown reduced viral load and increased CD_4^+ lymphocyte counts.[24] The introduction of these highly active antiretroviral therapies (HAART) arrested the progression of AIDS[25] and significantly reduced AIDS-related deaths in the United States and other industrialized nations. There is no doubt that HAART treatment regimens dramatically improved the quality of life and survival of patients infected with HIV, however, their ability to provide effective long-term antiretroviral therapy for HIV infection has become a complex issue. There are serious limitations with all of the currently approved protease inhibitors, including: 1) debilitating side effects and drug toxicities, 2) higher therapeutic doses due to "peptide-like" character, 3) expensive synthesis and high treatment cost, and most concerning, 4) the emergence of drug resistance. At least 40–50% of those patients who initially achieve favorable viral suppression to undetectable levels experience treatment failure.[26] Additionally, 20–40% of antiviral therapy-naive individuals infected with HIV-1 have persistent viral replication (plasma HIV RNA > 500 copies mL^{-1}) under HAART, possibly due to transmission of drug-resistant HIV-1 variants.[27] In addition to the issue of drug resistance, tolerance and adherence to complex medical regimens are becoming critical issues. The drugs must be taken in gram quantities daily because of low oral bioavailability. Most currently approved PIs are associated with complex side effects including peripheral lipodystrophy, hyperlipidemia, and insulin resistance. Thus, current designs and syntheses of a new class of PIs are faced with the following major challenges: 1) improvement of potency and pharmacokinetic properties which can substantially reduce therapeutic doses, maximize effectiveness, and reduce side effects; 2) design of inhibitors that can effectively combat drug resistance; and 3) cost-effective synthesis of PIs to make these drugs readily accessible to third world countries, where the epidemic continues to worsen. To address various issues of PI therapy, our research emphasis has been focused on the design and synthesis of nonpeptidal protease inhibitors that are potent against mutant strains resistant to the currently approved protease inhibitors.

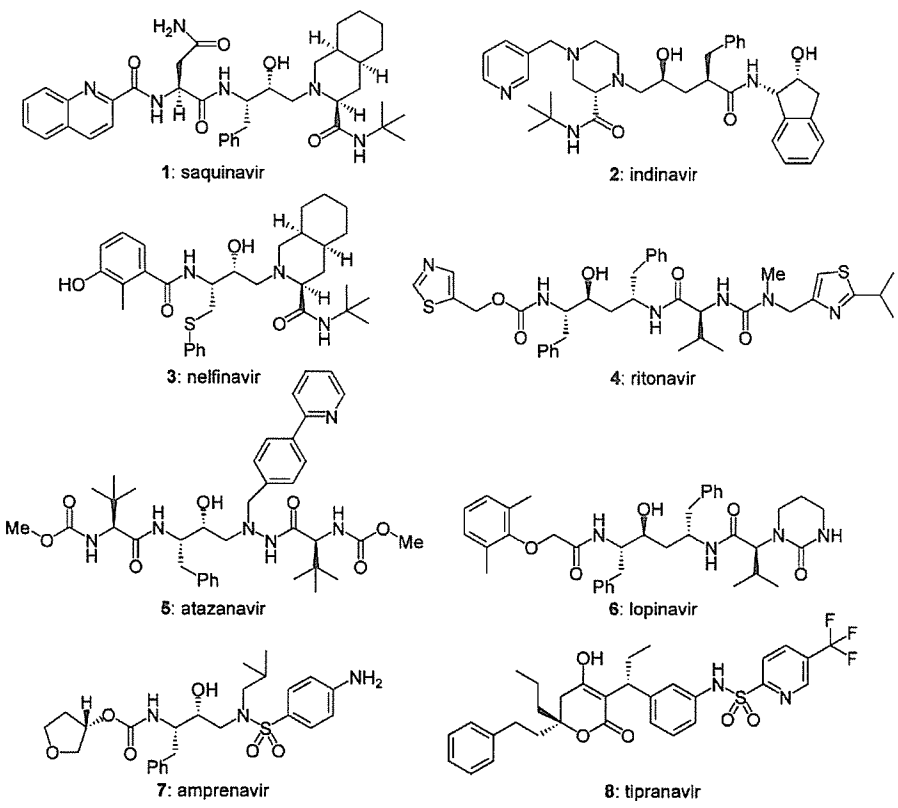

Figure 1. FDA-approved HIV protease inhibitors for the treatment of HIV infection and AIDS.

Structure-Based Design of Cyclic-Ether-Derived Nonpeptide P_2 Ligands

In an effort to reduce peptidic features, molecular weight, and structural complexity of the current protease inhibitors, we have designed a number of nonpeptidal high-affinity ligands for the HIV protease substrate binding site. The ligands are specifically designed based on various available three-dimen-

sional structures of the protein–ligand complex. One of the important elements in this design is to incorporate a stereochemically defined and conformationally constrained cyclic ether that will replace peptide bonds, mimic the biological mode of action, and make maximum interactions in the active site including hydrogen bonding with the protein backbone. The idea of incorporating cyclic ethers is from the observation that a number of naturally occurring biologically active motifs comprise cyclic ether as one of their epitopes. On the basis of this presumption, Ghosh et al. developed 3′-tetrahydrofuranylglycine[28] as a novel P_2 substitute for the asparagine side chain in saquinavir (**1**). This inhibitor (compound **9**) reproducibly showed a 4-fold higher potency ($IC_{50}=0.054\pm0.027$ nM) than saquinavir ($IC_{50}=0.23\pm0.1$ nM). Inhibitor **9** ($CIC_{95}=8$ nM) also showed consistent 3-fold higher CIC_{95} potency over saquinavir ($CIC_{95}=22$ nM). Further removal of the P_3 quinaldic amide ligand in **9** and incorporation of a stereochemically defined 3-tetrahydrofuran urethane functionality as a P_2 ligand provided inhibitor **10** ($IC_{50}=160$ nM and $CIC_{50}=800$ nM). The importance of the cyclic ether was further demonstrated in hydroxyethylene isostere-derived HIV protease inhibitors containing a 3-(*S*)-tetrahydrofuran urethane as the high-affinity P_2 ligand (Figure 2).[29] Inhibitor **11** has shown a 5000-fold enhancement in potency relative to inhibitor **10**.

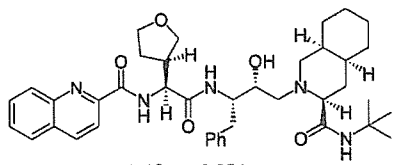

9: IC_{50} = 0.054 nM
CIC_{95} = 8 nM

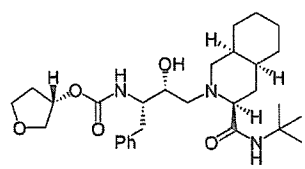

10: IC_{50} = 160 nM
CIC_{95} = 800 nM

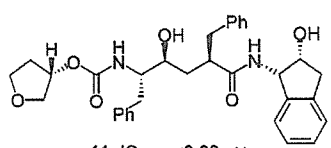

11: IC_{50} = <0.03 nM
CIC_{95} = 3 nM

Figure 2. Hydroxyethylene- and hydroxyethylamine-derived inhibitors.

Researchers at Vertex laboratories developed a significantly lower-molecular-weight protease inhibitor that incorporates 3-(*S*)-tetrahydrofuran as the P_2 ligand and an (*R*)-(hydroxyethyl)-sulfonamide as the isostere **12**.[30] This afforded the highly potent inhibitor VX-476, which was subsequently renamed amprenavir[21] (**7**, Figure 3) and approved by the FDA for the treatment of HIV infection and AIDS. The crystal structure of amprenavir-bound HIV protease revealed the extensive interactions

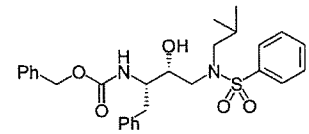

12: K_i = 3.2 nM
EC_{50} = 113 nM

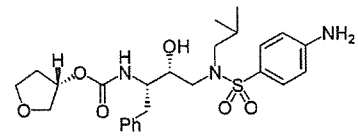

7: amprenavir
K_i = 0.6 nM
IC_{90} = 40 nM

Figure 3. Urethane-based HIV protease inhibitors.

of the ring oxygen atom of the 3-(*S*)-tetrahydrofuryloxy group. This O atom is apparently involved in a weak interaction with the Asp 29 and Asp 30 backbone amides (at 3.4 and 3.5 Å, respectively).

Development of Bis-THF as a privileged P_2 Ligand

Our structure-based design effort led to the development of a number of cyclic-ether-derived nonpeptide P_2 ligands for the HIV protease substrate binding site. Particularly notable is the potency-enhancing effect of the (3*S*)-tetrahydrofuranyl urethane in inhibitors that contain a hydroxyethylene or a hydroxyethylsulfonamide isostere. As mentioned above, a protein–ligand X-ray crystal structure indicated hydrogen bonding between the tetrahydrofuran (THF) group and the main-chain aspartic acids (Asp 29 and Asp 30), as well as van der Waals interactions in the S_2 site. Our design effort then concentrated on further improving the potency of inhibitor **10** (Figure 2) which contains (3*S*)-tetrahydrofuranyl urethane in the saquinavir-derived hydroxyethylamine isostere. Our objective was to design a ligand that would maximize the hydrophobic and hydrogen bonding interactions with the residues in the S_2 site. To this end, we further explored the use of a polyether template to mimic the peptide region that binds to the viral enzyme. After careful analysis of the X-ray crystal structure of the saquinavir-bound protease, we speculated that exchange of the (3*S*)-tetrahydrofuran moiety for a fused bicyclic tetrahydrofuran (bis-THF) derivative could effectively hydrogen bond to the NH groups of Asp 29 and Asp 30. The conformationally constrained bis-THF should also offset the loss of P_3 hydrophobic binding of the quinoline ring in saquinavir. However, with the ultimate goal of producing high-affinity P_2 ligand, we actually designed and synthesized a new class of cyclic fused bis-THF[31] urethane-based HIV protease inhibitors. The inhibitor **13**, which incorporates (3*R*,3a*S*,6a*R*)-bis-THF as the P_2 ligand, exhibited a significant improvement in enzyme inhibitory and antiviral potency. Inhibitor **13** has shown enzyme inhibitory activity (IC_{50}) of 1.8 nM and a CIC_{95} value of 46 nM (Figure 4). Furthermore, inhibitor **13** has shown improved aqueous solubility, decreased

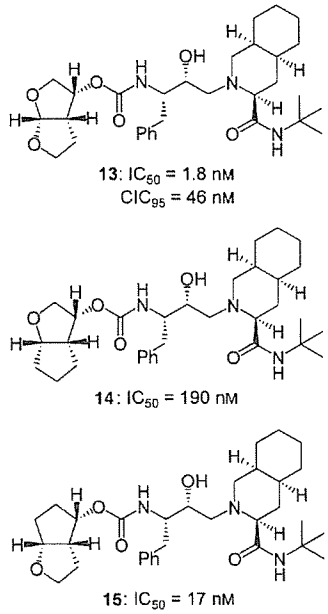

Figure 4. Bis-THF-urethane-based HIV protease inhibitors.

log*P* values, and is lower in molecular weight than saquinavir. Detailed SAR studies indicate that stereochemistry, placement of the oxygen atoms, ring size, and substituents are all essential to optimum binding.

Compared with THF-based inhibitor **10**, bis-THF inhibitor **13** showed nearly 90-fold enhancement in its inhibitory potency and greater than 15-fold enhancement in its antiviral potency. The X-ray crystal structure of **13**-bound protease provided important molecular insight into the ligand binding site interactions. In particular, the bis-THF ring oxygen atoms effectively participate in the same binding site as the P_2 asparagine carboxamide and the P_3 quinaldic amide carbonyl groups of inhibitor **1**. As expected, both oxygen atoms in the bis-THF ligand are involved in hydrogen bonding interactions with the Asp29 and Asp30 NH groups present in the S_2 subsite of the protease.

Our initial synthesis of the optically active bis-THF ligand from (*R*)-malic acid was far from satisfactory for carrying out detailed SAR studies.[31a] Our subsequent three-step synthesis of racemic bis-THF followed by lipase-catalyzed efficient optical resolution broaden the scope and utility of this novel polyether-like nonpeptide ligand.[32] Incidentally, the bis-THF ligand is also a subunit of ginkgolides A–C, an important class of natural products with significant biological activities.[33,34] Other economical syntheses of bis-THF ligands have been reported in recent years.[35]

Development of UIC-94003 (TMC-126) and UIC-94017 (TMC-114)

Following discovery of the bis-THF ligand while replacing two amide bonds and the 10π-quinaldic acid amide of saquinavir, we investigated the potential of this ligand in conjunction with a hydroxyethyl(sulfonamide) isostere. As shown in Figure 5, incorporation of (3*R*,3a*S*,6a*R*)-bis-THF as a P_2 ligand and *p*-methoxybenzenesulfonamide as the P_2' ligand provided

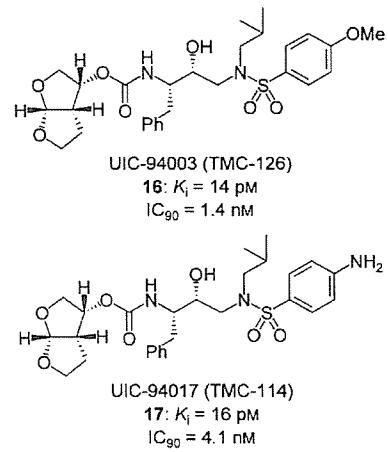

Figure 5. Bis-THF-derived inhibitors TMC-126 and TMC-114.

inhibitor **16** (UIC-94003, K_i = 14 pM, IC_{90} = 1.4 nM). Similarly, incorporation of a P_2' *p*-aminobenzenesulfonamide provided inhibitor **17** (UIC-94017, K_i = 16 pM, IC_{90} = 4.1 nM). Both inhibitors exhibited remarkable enzyme inhibitory and antiviral properties.[36]

Inhibitors **16** and **17** were subsequently named TMC-126 and TMC-114, respectively. The in vitro drug-sensitivity studies using HIV-1 laboratory isolates indicated that **16** is one of the most potent inhibitors of wild-type HIV protease. In addition, it was shown to be potent against a wide spectrum of recombinant HIV protease-containing HIV-1 variants that were highly cross-resistant to one or more of the protease inhibitors used in first-line therapy. As can be observed in Table 1, the initial in vitro drug-sensitivity study of **16** with the HIV-1 laboratory isolates HIV-1_{LAI} and HIV-$1_{Ba\text{-}L}$ in PHA-PBMC, or HIV-2_{EHO} in MT-2 cells showed that **16** was >10-fold more potent than five currently available protease inhibitors (RTV, IDV, SQV, NFV, and APV) against HIV-1_{LAI} and HIV-$1_{Ba\text{-}L}$ (IC_{50} = 0.3 nM).[37]

Inhibitor **16** also exhibited remarkably potent and unprecedented broad-spectrum activity against a wide range of primary, multidrug-resistant HIV-1 strains isolated from patients with AIDS who had failed 9 to 11 anti-HIV-1 drugs. The results are shown in Table 2. These HIV-1 strains contained 9–14 amino acid substitutions in the protease-encoding region and are known to exert resistance against currently approved protease inhibitors (RTV, IDV, SQV, NFV, and APV). As can be observed in Table 2, all strains had a higher level of resistance (6- to >77-fold) to RTV, IDV, NFV, and APV than the wild-type clinical strain HIV-$1_{ERS104pre}$. Very impressively, TMC-126 suppressed all eight isolates with IC_{50} values ranging from 0.5 to 5 nM.

The inhibitory activity of **16** against wild-type HIV-1 and various mutant proteases is given in Table 3. Vitality was determined from the measured K_i values, and the data indicate that inhibitor **16** possesses highly potent and unprecedented broad-spectrum antiretroviral activity.[38]

Table 1. Sensitivity of HIV-1_{LAI}, HIV-1_{Ba-L}, and HIV-2_{EHO} to various PIs.

Virus	Cell	IC_{50} [nM][a] Ritonavir (RTV)	Indinavir (IDV)	Saquinavir (SQV)	Nelfinavir (NFV)	Amprenavir (APV)	UIC-94003 (TMC-126)
HIV-1_{LAI}	PBMC	40±0.8	15±0.4	11±0.5	9±0.03	17±0.3	0.3±0.09
HIV-1_{Ba-L}	PBMC	38±2	17±0.1	14±1	3±0.2	23±0.9	0.3±0.04
HIV-1_{LAI}	MT-2	41±0.5	19±0.9	23±0.2	5±0.2	41±1	0.3±0.1
HIV-2_{EHO}	MT-2	350±2.5	10±0.4	4±0.05	20±1	530±3	0.5±0.07

[a] Data represent mean values ±SD derived from the results of three independent experiments conducted in duplicate or triplicate. For PBMC (peripheral blood mononuclear cells), IC_{50} values were determined by using PHA-PBMC exposed to each HIV-1 preparation (50×$TCID_{50}$ per 10^5 PBMC) in the presence of each anti-HIV-1 agent and by using the inhibition of p24 Gag protein production as an endpoint on day 7 of culture ($TCID_{50}$= 50% tissue culture infective dose). MT-2 cells (2×10^3) were exposed to 100 $TCID_{50}$ of HIV-1_{LAI} or HIV-2_{EHO} and cultured in the presence of various concentrations of PIs, and the IC_{50} values were determined using the MTT assay on day 7 of culture. (MTT = 3-[4,5-dimethylthiazol-2-yl]-2,5-diphenyltetrazolium bromide.)

Upon selection of HIV-1 in the presence of TMC-126, mutants carrying a novel active site mutation A28S appeared along with L10F, M46I, I50V, A71V and N88V. The drug-sensitivity results of TMC-126-selected HIV-1 strains to PIs are described in Table 4. These results indicate that with IC_{50} values as low as 0.02 μM, TMC-126 suppressed the replication of HIV-1 variants selected with 62 and 30 passages in the presence of increasing concentrations of TMC-126 and amprenavir, respectively. Our detailed studies and data have provided firm evidence that TMC-126 has significant advantages over other protease inhibitors.

Inhibitor **17**, which is structurally related to **16**, has also shown similar antiviral activity and resistance profiles. However, **17**, with a basic P_2' amine functionality, has shown favorable pharmacokinetic properties in animals. It was subsequently selected for clinical development and underwent multicenter clinical trials.[39]

Recently, we demonstrated that **17** exerts more potent activity against a laboratory HIV-1 strain, HIV-1_{LAI}, relative to the activities of the currently available FDA-approved protease inhibitors (Table 5). The six available protease inhibitors (SQV, APV, IDV, NFV, RTV, and LPV) suppressed the infectivity and replication of HIV-1_{LAI}, with IC_{50} values ranging from 0.017 to 0.047 μM in MT-2 cells, whereas TMC-114 had the most potent activity in terms of suppressing the infectivity and replication of the virus (IC_{50} = 0.003 μM).[40]

Inhibitor **17** was further tested against R5 laboratory HIV-1 strain, HIV-1_{Ba-L}, and two HIV-2 strains, HIV-2_{ROD} and HIV-2_{EHO} in vitro. It was also found that **17** had greater activities (6- to 13-fold) against HIV-1_{Ba-L} than the other tested protease inhibitors. In addition, **17** had more potent activity than the other four protease inhibitors against two HIV-2 strains, suppressing their infectivity and replication (Table 6).

Table 3. Enzyme inhibitory potency of **16** against wild-type and mutant proteases.

Enzyme	K_i [pM]	$K_{i(WT)}/K_{i(mutant)}$	Vitality
WT	14	1	1
D30N	<5	0.33	0.3
V32I	8	0.57	0.5
I84V	40	2.85	1
V32I/I84V	70	5	0.7
M46F/V82A	<5	0.33	0.1
G48V/L90M	<5	0.33	0.1
V82F/I84V	7	0.5	0.1
V82T/I84V	22	1.57	0.1
V32I/K45I/F53L/A71V/I84V/L89M	31	2.2	0.1
V32I/L33F/K45I/F53L/A71V/I84V	46	3.3	0.1
K20R/M36I/I54V/A71V/V82T	31	2.2	0.1

Table 2. PI sensitivity of HIV-1 isolated from heavily drug-experienced individuals.

Virus	Amino Acid Substitution[a]	IC_{50} [μM][c] RTV	IDV	SQV	NFV	APV	TMC-126
WT[b]	L63P	0.044 (1)	0.013 (1)	0.010 (1)	0.023 (1)	0.025 (1)	0.0007 (1)
1	L10I, K14R, L33I, M36I, M46I, F53L, K55R, I62V, L63P, A71V, G73S, V82A, L90M, I93L	>1 (>23)	>1 (>77)	0.27 (27)	>1 (>43)	0.27 (11)	0.004 (6)
2	L10I, I15V, K20R, M36I, M46L, I54V, K55R, I62V, L63P, K70Q, V82A, L89M	>1 (>23)	0.49 (38)	0.037 (4)	0.33 (14)	0.28 (11)	0.0013 (2)
3	L10I, I15V, E35D, N37E, K45R, I54V, L63P, A71V, V82T, L90M, I93L, C95F	>1 (>23)	0.49 (38)	0.036 (4)	>1 (>43)	0.26 (10)	0.001 (1)
4	L10I, V11I, T12E, I15V, L19I, R41K, M46L, L63P, A71T, V82A, L90M	>1 (>23)	0.21 (16)	0.033 (3)	0.09 (4)	0.31 (12)	0.0016 (2)
5	L10I, K43T, M46L, I54L, L63P, A71T, V82A, L90M, Q92K	>1 (>23)	>1 (>77)	0.31 (31)	0.41 (18)	0.67 (27)	0.0024 (3)
6	L10I, K14R, R41K, M46L, I54V, L63P, A71V, V82A, L90M, I93L	>1 (>23)	0.30 (23)	0.19 (19)	>1 (>43)	0.16 (6)	0.0005 (1)
7	L10I, L24I, L33F, E35D, M36I, N37S, M46L, I54V, R57K, I62V, L63P, A71V, G73S, V82A	>1 (>23)	>1 (>77)	0.12 (12)	>1 (>43)	0.49 (20)	0.0055 (8)
8	L10R, N37D, M46I, I62V, L63P, A71V, G73S, V77I, V82T, L90M, I93L	>1 (>23)	0.55 (42)	0.042 (4)	>1 (>43)	0.15 (6)	0.001 (1)

[a] In PR. The amino acid sequence of each viral isolate was deduced from the nucleotide sequence and compared with the consensus B sequence cited from the Los Alamos data base. [b] A clinical isolate, HIV-$1_{ERS104pre}$, served as a source of wild-type (WT) HIV-1. [c] IC_{50} values were determined by using PHA-PBMC exposed to HIV-1 strains (50×$TCID_{50}$ per 10^5 PBMC) in the presence of each anti-HIV-1 agent and by using the inhibition of p24 Gag protein production as an endpoint. All values were determined in triplicate, and those shown are representative of two or three separate experiments. Numbers in parentheses represent the fold change of IC_{50} values against each isolate compared with the IC_{50} against HIV-1 wild-type.

Table 4. Amino acid substitution in PR and sensitivity of drug-resistant HIV-1 strains to PIs.[a]

Virus	Amino Acid Substitution	IC_{50} [μM]					
		RTV	IDV	SQV	NFV	APV	TMC-126
$HIV\text{-}1_{NL4\text{-}3}$	-	0.038 (1)	0.011 (1)	0.019 (1)	0.023 (1)	0.042 (1)	0.0003 (1)
$HIV\text{-}1_{UIC\text{-}P62}$	L10F, A28S, M46I, I50V, A71V, N88D	0.055 (1)	0.08 (7)	0.01 (1)	0.11 (5)	0.83 (20)	0.021 (70)
$HIV\text{-}1_{APVP30}$	L10F, V32I, K20R, M36I, M46I, I54M, A71V, I84V	>1 (>26)	0.32 (30)	0.035 (2)	>1 (43)	>1 (>25)	0.029 (100)

[a] MT-2 cells (2×10^3) were exposed to $HIV\text{-}1_{NL4\text{-}3}$, $HIV\text{-}1_{UIC\text{-}P62}$, (HIV-1 following 62 passages in the presence of increasing concentrations of TMC-126), or $HIV\text{-}1_{APV\text{-}P30}$ (HIV-1 following 30 passages in the presence of increasing concentrations of APV, all $100\times TCID_{50}$) and cultured in the presence of various drug concentrations. The IC_{50} values were determined on day 7 of culture in the MTT assay. All values were determined in duplicate, and those shown are representative of two or three independent experiments. The numbers in the parentheses represent fold changes relative to $HIV\text{-}1_{NL4\text{-}3}$ (wild-type).

Table 5. Cytotoxicity and activity of UIC-94017 (TMC-114) against $HIV\text{-}1_{LAI}$.[a]

Drug	IC_{50} [μM]	CC_{50} [μM]	Selectivity Index
TMC-114	0.003 ± 0.0001	74.4 ± 1.2	24800
SQV	0.017 ± 0.003	11.3 ± 2.8	660
APV	0.036 ± 0.011	>100	>2800
IDV	0.047 ± 0.008	70.3 ± 4.6	1500
NFV	0.027 ± 0.004	ND	ND
RTV	0.045 ± 0.012	ND	ND
LPV	0.034 ± 0.006	ND	ND

[a] MT-2 cells (2×10^3) were exposed to $100\times TCID_{50}$ of $HIV\text{-}1_{LAI}$ and cultured in the presence of various concentrations of PIs. The IC_{50} values were determined with the MTT assay on day 7 of culture. All assays were conducted in duplicate, and the data shown represent the mean ± SD from the results of three independent experiments (ND: not determined). [b] Concentration that causes 50% cytotoxicity.

Further tests on the activity of **17** and the five clinically available PIs revealed that **17** effectively blocked the infectivity and replication of each of the $HIV\text{-}1_{NL4\text{-}3}$ variants exposed to and selected for resistance to SQV, IDV, NFV, or RTV at concentrations up to 5 μM (Table 7).[40] Also, **17** exerted potent activity against highly multi-PI-resistant clinical HIV-1 variants isolated from seven patients with AIDS who had no response to existing antiviral regimens after having received a variety of antiviral agents (Table 8).

One of our guiding principles to combat drug resistance is to design ligands and incorporate structural features in the inhibitors to maximize the interactions in the active site of HIV protease. In particular, we strive toward making extensive hydrogen bonding interactions with the protein backbone. As there is only a small distortion between the backbone conformations of protein–ligand complexes of wild-type HIV protease

Table 6. Activities of selected anti-HIV agents against $HIV\text{-}1_{Ba\text{-}L}$, $HIV\text{-}2_{ROD}$, and $HIV\text{-}2_{EHO}$.

Virus	Cell	IC_{50} [μM][a]						
		AZT	SQV	APV	IDV	NFV	RTV	TMC-114
$HIV\text{-}1_{Ba\text{-}L}$[b]	PBMC	0.009 ± 0.001	0.018 ± 0.010	0.026 ± 0.005	0.025 ± 0.012	0.017 ± 0.004	0.039 ± 0.020	0.003 ± 0.0003
$HIV\text{-}2_{ROD}$[c]	MT-2	0.018 ± 0.002	0.003 ± 0.0002	0.23 ± 0.01	0.014 ± 0.006	0.019 ± 0.003	0.13 ± 0.06	0.003 ± 0.0001
$HIV\text{-}2_{EHO}$[c]	MT-2	0.011 ± 0.002	0.006 ± 0.002	0.17 ± 0.05	0.011 ± 0.002	0.029 ± 0.018	0.24 ± 0.006	0.006 ± 0.003

[a] All assays were conducted in duplicate or triplicate, and the data shown represent the mean ± SD derived from the results of three independent experiments. [b] IC_{50} values were determined with PHA-PBMC and the inhibition of p24 Gag protein production by the drug as an endpoint. [c] MT-2 cells were exposed to the virus, cultured, and the IC_{50} values were determined by MTT assay.

Table 7. Activity of TMC-114 against laboratory PI-resistant HIV-1.

Virus	Amino Acid Substitution[a]	IC_{50} [μM][b]					
		SQV	APV	IDV	NFV	RTV	TMC-114
$HIV\text{-}1_{NL4\text{-}3}$	WT	0.009 (1)	0.027 (1)	0.011 (1)	0.020 (1)	0.018 (1)	0.003 ± 0.0005 (1)
$HIV\text{-}1_{SQV5\mu M}$	L10I, G48V, I54V, L90M	>1 (>111)	0.17	>1 (>91)	0.30 (15)	>1 (>56)	0.005 ± 0.0009 (2)
$HIV\text{-}1_{APV5\mu M}$	L10F, V32I, M46I, I54M, A71V, I84V	0.020 (2)	>1 (>37)	0.31 (28)	0.21 (11)	>1 (>56)	0.22 ± 0.05 (73)
$HIV\text{-}1_{IDV5\mu M}$	L10F, L24I, M46I, L63P, A71V, G73S, V82T	0.015 (2)	0.33 (12)	>1 (>91)	0.74 (37)	>1 (>56)	0.029 ± 0.0007 (10)
$HIV\text{-}1_{NFV5\mu M}$	L10F, D30N, K45I, A71V, T74S	0.031 (3)	0.093 (3)	0.28 (25)	>1 (>50)	0.09 (5)	0.003 ± 0.0002(1)
$HIV\text{-}1_{RTV5\mu M}$	M46I, V82F, I84V	0.013 (1)	0.61 (23)	0.31 (28)	0.24 (12)	>1 (>56)	0.025 ± 0.006 (8)

[a] In PR. [b] MT-4 cells (10^4) were exposed to each HIV-1 ($100\times TCID_{50}$), and the inhibition of p24 Gag protein production by the drug was used as an endpoint. Numbers in parentheses represent the fold change in IC_{50} for each isolate relative to that of $HIV\text{-}1_{NL4\text{-}3}$. The data represent the mean ± SD from the results of three independent experiments conducted in triplicate.

Table 8. Activity of TMC-114 against HIV-1 clinical isolates in PHA-PBMC.[a]

Virus	IC_{50} [μM]						
	AZT	SQV	APV	IDV	NFV	RTV	TMC-114
HIV-$1_{ERS104pre}$ (WT X4)	0.004	0.010	0.023	0.018	0.019	0.027	0.003
HIV-1_{MOKW} (WT R5)	0.016	0.004	0.011	0.018	0.033	0.032	0.003
HIV-1_{TM} (MDR X4)	0.73 (183)	0.23 (23)	0.39	>1 (>56)	0.54 (28)	>1 (>37)	0.004 (1)
HIV-1_{MM} (MDR R5)	0.37 (93)	0.30 (30)	0.34	>1 (>56)	>1 (>53)	>1 (>37)	0.02 (7)
HIV-1_{JSL} (MDR R5)	0.08 (20)	0.35 (35)	0.75 (33)	>1 (>56)	>1 (>53)	>1 (>37)	0.029 (10)
HIV-1_{A} (MDR X4)	ND	0.14 (14)	0.16 (7)	>1 (>56)	0.36 (19)	>1 (>37)	0.004 (1)
HIV-1_{B} (MDR X4)	ND	0.31 (31)	0.34 (15)	>1 (>56)	>1 (>53)	>1 (>37)	0.013 (4)
HIV-1_{C} (MDR X4)	ND	0.037 (4)	0.28 (12)	>1 (>56)	0.44 (23)	>1 (>37)	0.003 (1)
HIV-1_{G} (MDR X4)	ND	0.029 (3)	0.25 (11)	0.39 (22)	0.32 (17)	0.44 (16)	0.004 (1)

[a] The amino acid substitutions identified in the PR-encoding region of HIV-$1_{ERS104pre}$, HIV-1_{TM}, HIV-1_{MM}, HIV-1_{JSL}, HIV-1_{A}, HIV-1_{B}, HIV-1_{C}, and HIV-1_{G} relative to the consensus type B sequence cited from the Los Alamos database include: L63P (HIV-$1_{ERS104pre}$); L10I, K14R, R41K, M46L, I54V, L63P, A71V, V82A, L90M, and I93L (HIV-1_{TM}); L10I, K43T, M46L, I54V, L63P, A71V, V82A, L90M, and Q92K (HIV-1_{MM}); L10I, L24I, L33F, E35D, M36I, N37S, M46L, I54V, R57K, I62V, L63P, A71V, G73S, and V82A (HIV-1_{JSL}); L10I, I15V, E35D, N37E, K45R, I54V, L63P, A71V, V82T, L90M, I93L, and C95F (HIV-1_{A}); L10I, K14R, L33I, M36I, M46I, F53I, K55R, I62V, L63P, A71V, G73S, V82A, L90M, and I93 (HIV-1_{B}); L10I, I15V, K20R, L24I, M36I, M46L, I54V, I62V, L63P, K70O, V82A, and L89M (HIV-1_{C}); and L10I, V11I, T12E, I15V, L19I, R41K, M46L, L63P, A71T, V82A, and L90M (HIV-1_{G}). HIV-1_{MOKW} was confirmed to lack any known drug-resistance-associated amino acid substitutions. IC_{50} values were determined by using PHA-PBMC as target cells and the inhibition of p24 Gag protein production as an endpoint. All values were determined in triplicate, and those shown are derived from the results of three independent experiments. Numbers in parentheses represent the fold change in IC_{50} values for each isolate relative to those of HIV-$1_{ERS104pre}$. MDR = multidrug resistant; ND = not determined.

and mutant HIV proteases,[41] it is conceivable that such backbone hydrogen bonding interactions can be maintained with the mutant proteases. Our design of inhibitor **17** is based on this hypothesis. To investigate the mechanism by which **17** exerts its potent activity against a wide spectrum of multi-PI-resistant HIV-1 strains, an X-ray crystal structure of HIV-1 protease complexed with **17** at 1.30 Å resolution was examined.[42] It was found that the two oxygen atoms of the bis-THF groups of **17** formed strong hydrogen bonds with the main chains of Asp 29 and Asp 30 in the S_2 subsite (Figure 6). It was also found that **17** formed new polar interactions with the amide of the main chain and the carboxylate oxygen atom of Asp 30. These interactions are proposed to be crucial and could be the reason for potent activity against multi-PI-resistant variants.[43] Its highly potent antiviral activity against wild-type HIV-1 isolates and a large panel of PI-resistant viruses, as well as its pharmacokinetic properties made inhibitor **17** the choice as a candidate for development and further clinical studies. Inhibitor **17** has subsequently been renamed darunavir.

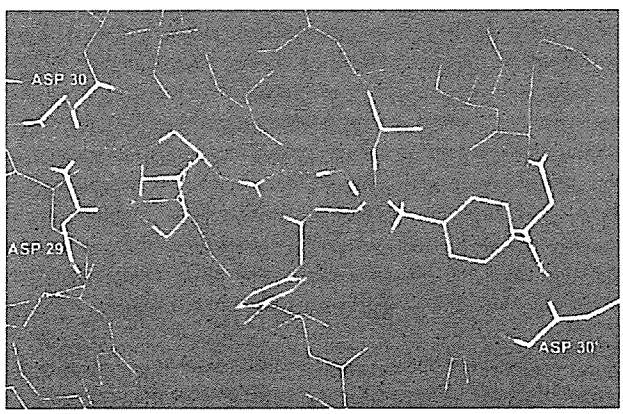

Figure 6. Hydrogen bond interactions of HIV protease with **17** (TMC-114, darunavir).

Preclinical Results of TMC-114 (Darunavir)

TMC-114 exhibited the following characteristics in our assay: antiviral $IC_{50} = 4.7$ nM, $IC_{90} = 10.3$ nM, $CC_{50} > 100$ μM in a cell culture assay. TMC-114 was tested against a panel of 20 HIV variants resistant to current protease inhibitors, but there was no greater than a 5-fold increase in IC_{50} values. The observed IC_{50} values were < 100 nM against 100% ($IC_{50} < 10$ nM against 94%) of 261 randomly selected, recent recombinant clinical isolates, among which 32% show a ≥ 10-fold increase in IC_{50} for at least one of the current PIs. Good relative stability upon incubation with human liver microsomes was demonstrated. This inhibitor maintains high blood levels in dogs at an oral dose of 20 mg kg^{-1} body mass (C_{max} plasma concentrations of 13.7 μM). It has shown excellent potency ($IC_{50} < 10$ nM) against clinical HIV-1 isolates that exhibit resistance to currently approved protease inhibitors.[44]

A randomized, double-blind, placebo-controlled, dose-escalating trial was performed to examine the safety, tolerability, and pharmacokinetics of single oral doses of inhibitor **17** (TMC-114). Two panels of nine healthy volunteers (six active, three placebo) received alternating doses of 100, 200, 400, 800, 1200, or 1600 mg. Because the maximum tolerated dose was not reached, additional doses were added to administer 2400, 3200, and 4000 mg. Initially, plasma concentrations increased greater than proportional with the dosing. No further increases were observed between 2400 and 3200 mg. The mean C_{max} was 14.4–15.3 μg mL^{-1} (26.2–27.8 μM) at these dose levels. The elimination half-life was approximately 10 h, irrespective of dose. For doses of 800 mg and greater, plasma levels at 8–12 h post-dose exceeded protein-adjusted IC_{50} values for isolates resistant to currently approved PIs. All doses were considered safe. Diarrhea, related to polyethylene glycol (PEG) in the formulation, occurred at high dose levels and limited further escalation. Short-term localized paresthesia (oral, 3; fingers, 1) was observed in four out of six subjects at the 3200 mg dose. These studies demonstrated that single doses of **17** were safe and well-tolerated at all doses tested. The maximum tolerated dose was not achieved. Further dose increases were hindered by solvent-related diarrhea. Single-dose plasma levels provided superior inhibitory quotients for PI-resistant HIV-1 isolates over

currently approved protease inhibitors. Tibotec (Belgium) has carried out clinical development of darunavir (TMC-114).[39] Recently, the FDA has approved darunavir for treatment of drug-resistant HIV.[45]

Recently, researchers at Tibotec made the effort to confirm and further examine the antiviral activity (against both wild-type and PI-resistant HIV), cytotoxicity, and mechanism of action of TMC-114.[46] The results of in vitro studies of TMC-114 against different laboratory HIV strains revealed potent anti-HIV activity, with IC_{50} values in the range of 1–5 nM and corresponding IC_{90} values in the range of 2.7–13 nM. In terms of cytotoxicity, TMC-114 exhibited no cytotoxicity at concentrations up to 100 μM, and the selectivity index was found to be >20000 for wild-type HIV-1. In addition, TMC-114 was equally active against 32 recombinant strains from clinical isolates. The effect of human serum and alpha-1-acid glycoprotein (AAG) on the antiviral activity of TMC-114 and other approved PIs at 0.5–5 μM showed a <7-fold decrease in potency, pointing to a saturable binding of PIs to AAG. The activity studies against PI-resistant HIV-1 variants, in a panel of 17 recombinant clinical isolates carrying multiple protease mutations and demonstrating resistance to an average of five other PIs, were susceptible to TMC-114, defined as a fold change in IC_{50} of <4. TMC-114 was also effective against the majority of 1501 PI-resistant recombinant viruses derived from recent clinical samples with IC_{50} values of <10 nM for 75% of the samples. Isothermal titration calorimetry also showed very high-affinity binding (K_d = 0.0045 nM) of TMC-114 to HIV-1 protease. X-ray crystallographic analysis confirmed that TMC-114 forms strong hydrogen bonds with residues in the main chain of the protease active site (Asp29 and Asp30).[42]

Exploration of P_2' Ligand Functionalities

We further incorporated a number of other functionalities at the P_2' sulfonamide to interact specifically with residues in the enzyme active site. The results are reported herein for the first time.[38a] Based on the X-ray crystal structure of HIV-1 protease bound to inhibitor **1**, various functionalities on the sulfonamide ligands can form hydrogen bonds with the backbone of Asp29′ and Asp30′. The X-ray crystal structure of HIV-1 protease bound to inhibitor **13** shows that, in some cases, there are favorable interactions with the side chain of Asp30′ as well.

A series of inhibitors (**18–22**) in Figure 7 have also shown exceedingly potent enzyme inhibition properties. Inhibitors **19**, **20**, and **21** were tested against proteases containing the noxious drug resistance associated mutations V82F/I84V and G48V/V82A. These inhibitors also possess broad-spectrum potent activity against mutant proteases. Inhibitor **22**, with a benzodioxanesulfonamide derivative as the P_2' ligand, has also exhibited marked enzyme inhibitory potency (<5 pM) and antiviral potency (IC_{50} = 1.1 nM in MT-2 cells). The antiviral potency of inhibitors **19–22** was determined with respect to wild-type clinical isolates HIV-1_{LAI} and HIV-$1_{Ba\text{-}L}$. The latter is a monocytotropic strain of HIV. The IC_{50} values for isolates HIV-1_{LAI} and HIV-$1_{Ba\text{-}L}$ were determined by exposing the PHA-simulated PBMC to

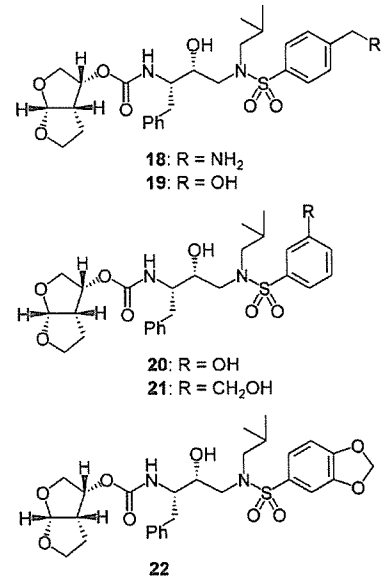

Figure 7. Bis-THF-based P_2' sulfonamide inhibitors.

HIV-1 (50×$TCID_{50}$ dose per 1×10^6 PBMC) in the presence of various concentrations of inhibitors **19–22**; the inhibition of p24 *gag* protein production was used as an endpoint on day 7 of culture ("p24 assay"). All drug sensitivities were performed in triplicate. The IC_{50} values for isolate HIV-1_{LAI} were also determined by exposing MT-2 cells (2×10^3) to 100×$TCID_{50}$ of HIV-1_{LAI} cultured in the presence of various concentrations of PIs.[47] The IC_{50} values were determined using the MTT assay on day 7 of culture. All sensitivities were determined in duplicate. The results are shown in Table 9. Thus, it appears that inhibitor **22** may exhibit a similar level of potency as inhibitor **16** (TMC-126) in various multidrug-resistant HIV strains.

Table 9. Antiviral potency of PIs **18–22**.

			IC_{50} [nM]				
Virus	Cell Type	Assay	**18**	**19**	**20**	**21**	**22**
HIV-1_{LAI}	MT-2	MTT	28	5.3	17	28	0.22
HIV-1_{LAI}	PBMC	p24	20	2.7	34	8	0.22
HIV-$1_{Ba\text{-}L}$	PBMC	p24	13	3	38	9.3	0.33

Bis-THF-Derived New Generation of HIV-1 Protease Inhibitors

Because of its extraordinary potency-enhancing effect and its ability to maintain potency against multi-PI-resistant isolates, the bis-THF ligand was incorporated into other isosteres. Abbott research group has recently disclosed the modification of ritonavir by incorporating bis-THF as the P_2 ligand.[48] The SAR studies of the conformationally constrained bis-THF P_2 ligand in combination with a dimethylphenoxyl acetate as a P_2' ligand yielded a series of potent HIV protease inhibitors, of which compounds **23** and **24** (Figure 8) have shown EC_{50} values of 31 and 76 nM, respectively, in the presence of human serum (50%).[48a]

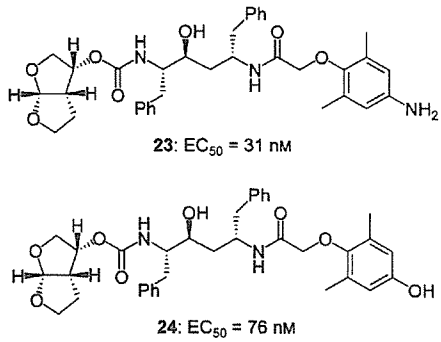

Figure 8. Abbott inhibitors with bis-THF in ritonavir isosteres.

GlaxoSmithKline researchers attempted further optimization of a hydroxyethylsulfonamide series of inhibitors by altering the substitutions on the P_1 and P_1' chains.[49] The structural modifications at the P_1' position resulted in highly potent molecules both in enzyme inhibition and antiviral assays. As shown in Figure 9, inhibitors **25** and **26** have shown enzyme inhibitory potency in the single-digit femtomolar (fM) range (**25** K_i = 10 fM and **26** K_i = 100 fM, Figure 9). These inhibitors also exhibited impressive antiviral potency.[49a]

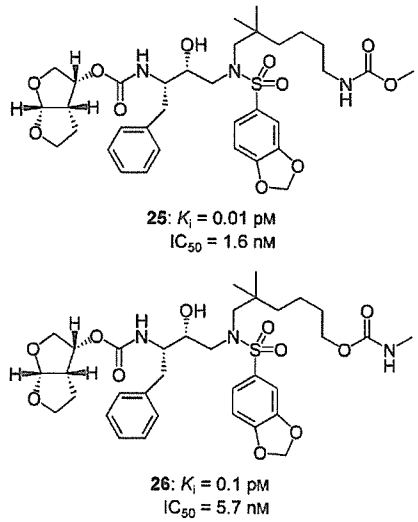

Figure 9. GlaxoSmithKline inhibitors with bis-THF and P_1' modification.

GlaxoSmithKline researchers further explored the structural modification of the P_1 ligand. They investigated tyrosine-derived inhibitors to achieve additional ligand–enzyme interactions. A number of remarkably potent inhibitors emerged from this investigation. As shown in Figure 10, inhibitors **27** and **28** have shown femtomolar enzyme inhibitory activity and very impressive antiviral activity.[50] However, SAR studies suggested that their activities are probably more a function of physicochemical parameters than any specific P_1 side-chain binding interactions. The heteroarylmethyl class of inhibitors **27** and **28** afforded the best activities overall, with single-digit nanomolar IC_{50} values against wild-type HIV virus (HXB2) and two multi-PI-

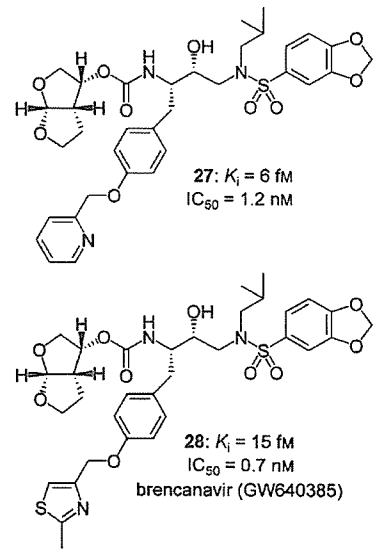

Figure 10. GlaxoSmithKline's bis-THF-based P_1 aryl derivatives.

resistant viruses (EP13 and D545701) in an MT-4 cell line. Compounds **27** and **28** were also found to have K_i values against wild-type HIV protease of 6 and 15 fM, respectively, which make these inhibitors 2400–6000-fold more potent than amprenavir.

As shown in Table 10, inhibitor **28** (GW640385) exhibited antiviral activity (IC_{50}) values of 0.7, 4.8, and 1.1 nM against HXB2, D545701, and EP13 viral strains, respectively.[50] The bioavailability of thiazole derivative **28** yielded 10% *F* and 20% *F* in rat and dog, respectively. Co-administration of 4 mg kg^{-1} of ritonavir with **28** improved oral bioavailability in rat and dog to 62% *F* and 86% *F*, respectively. These results led to the selection of GW640385 as a new clinical candidate.[50] Subsequently, **28** has been renamed brecanavir. Brecanavir has now advanced to Phase-III clinical development.

Tibotec researchers have extensively investigated TMC-126 (**16**) and TMC-114 (**17**).[51] Their efforts in modification of the P_2' sulfonamide ligand of TMC-114 led to the discovery of a new series of fused benzoxazole **29** and benzothiazole **30** sulfonamides (Figure 11).[52] Benzothiazole and benzoxazole inhibitors showed improved broad-spectrum antiviral activity in the range of 7.5–8.0 (pEC_{50}) against highly PI-resistant mutants.[52] Selected compounds have shown improved oral bioavailability (in silico and in vitro), solubility at different pH, permeability in Caco-2 assays, and metabolic stability in the presence of rat, dog, and human liver microsomes. Crystal structure determination, molecular modeling, and in vivo studies in rat and dog were performed to rationalize the broad-spectrum profiles of the antiviral activity of benzothiazole and benzoxazole inhibitors.

The crystal structure of HIV protease in complex with inhibitor **30** revealed the critical interactions associated with the P_2' surrogate and S_2' domain of the enzyme. The N atom of the thiazole ring in **30** interacts with the backbone NH group of Asp30′. The secondary amines present in both inhibitors **29**

Table 10. Resistance profile of **28** against a panel of PI-mutant viruses.

Virus	Mutations in PR	IC_{50} [nM][a]
WT HIV-1		0.7
468 APV-resistant	I15V, E34G, M36I, S37E, I50V, L63P	8.2
D545701 multi-PI-resistant	L10I, L19Q, K20R, E35D, M36I, S37N, M46I, I50V, I54V, I62V, L63P, A71V, V82A, L90M	4.8
14330 NFV-resistant	D30N, E35D, M36I, S37D, I62V, L64P, I64M, N88D	0.45
30813 IDV-resistant	I15V, I54V, R57K, I62V, L63P, H69Y, A71T, I72E, V82A, I85V	0.46
31246 multi-PI-resistant	L10I, I54V, L63P, A71V, I72V, V77I, V82A, I84V, L90M, Q92K	1.7
EP13 multi-PI-resistant	M46I, L63P, A71V, V82F, I84V	1.1
EP14 multi-PI-resistant	L10R, M46I, L63P, V82T, I85V	0.77
Triple multi-PI-resistant	M46I, I47V, I50V	5.4
I50V	I50V	1.6
I54V	I54V	0.22

[a] Determined in MT-4 cells.

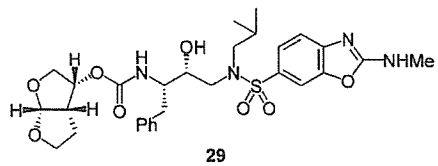

29

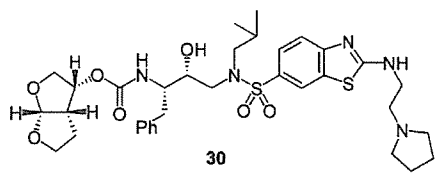

30

Figure 11. Tibotec's fused benzoxazole and benzothiazole analogues.

and **30** form a strong hydrogen bond with the side chain of Asp30′. Moreover, the pyrrolidine ring in inhibitor **30** is in close proximity to form a strong hydrogen bond with the Asp29′ side chain. These inhibitors are currently undergoing extensive preclinical investigation.

Conclusions

In summary, the structure-based design of bis-tetrahydrofuranyl urethane has emerged as a privileged nonpeptide P_2 ligand for a variety of highly potent HIV-1 protease inhibitors. Incorporation of this ligand provided HIV protease inhibitors with exceedingly potent antiviral activity and superior activity against multi-PI-resistant variants relative to other FDA-approved PIs. Recently, TMC-114 (darunavir) has been approved by the FDA for treatment of drug-resistant HIV. GW640385 (brecanavir), which incorporates bis-THF as the P_2 ligand, is currently in Phase-III clinical development. The bis-THF ligand has been specifically designed to fill in the hydrophobic S_2 pocket effectively and to promote extensive hydrogen bonding with the protein backbone in the enzyme S_2 site. The protein–ligand X-ray crystal structures with TMC-114 and other inhibitors with the bis-THF ligand revealed extensive interactions with the backbone of residues Asp29 and Asp30 at the S_2 site. The current design concept targeting the protein backbone may serve as an important guide to combat drug resistance. Further design and synthesis of conceptually novel inhibitors are in progress.

Acknowledgements

Financial support by the National Institutes of Health (GM 53386, A.K.G. and GM62920, I.T.W.) is gratefully acknowledged. This work was also supported in part by the Intramural Research Program of Center for Cancer Research, National Cancer Institute, National Institutes of Health and in part by a Grant-in-aid for Scientific Research (Priority Areas) from the Ministry of Education, Culture, Sports, Science, and Technology of Japan (Monbu Kagakusho), a Grant for Promotion of AIDS Research from the Ministry of Health, Welfare, and Labor of Japan (Kosei Rohdosho: H15-AIDS-001), and the Grant to the Cooperative Research Project on Clinical and Epidemiological Studies of Emerging and Re-emerging Infectious Diseases (Renkei Jigyo: No. 78, Kumamoto University) of Monbu-Kagakusho, the Georgia State University Molecular Basis of Disease Area of Focus, and the Georgia Cancer Coalition. We also thank Dr. Geoff Bilcer for helpful suggestions.

Keywords: AIDS chemotherapy · antiviral agents · bis-tetrahydrofuran · drug design · HIV protease inhibitors

[1] *UNAIDS/WHO Report on Annual AIDS Epidemic Update*, December **2005**. http://www.unaids.org/epi/2005/.
[2] J. Coffin, S. H. Hughes, H. E. Varmus, *Retroviruses*, Cold Spring Harbor, New York, **1997**.
[3] a) R. C. Gallo, S. Z. Salahuddin, M. Popovic, G. M. Shearer, M. Kaplan, B. F. Haynes, T. J. Palker, R. Redfield, J. Oleske, B. Safai, G. White, P. Foster, P. D. Markham, *Science* **1984**, *224*, 500–503; b) F. Barre-Sinoussi, J. C. Chermann, F. Rey, M. T. Nugeyre, S. Chamaret, J. Gruest, C. Dauguet, C. Axler-Blin, F. Vezinet-Brun, C. Rouzioux, W. Rozenbaum, L. Montagnier, *Science* **1983**, *220*, 868–871.
[4] a) M. C. Graves, J. J. Lim, E. P. Heimer, R. A. Kramer, *Proc. Natl. Acad. Sci. USA* **1988**, *85*, 2449–2453; b) W. G. Farmerie, D. D. Leob, N. C. Casavant, C. A. Hutchison, M. H. Edgell, R. Swanstorm, *Science* **1987**, *236*, 305–308.
[5] N. A. Roberts, J. A. Martin, D. Kinchington, A. V. Broadhurst, J. C. Craig, I. B. Duncan, S. A. Galpin, B. K. Handa, J. Kay, A. Krohn, R. W. Lambert, J. H. Merrett, J. S. Mills, K. E. B. Parkes, S. Redshaw, A. J. Ritchie, D. L. Taylor, G. J. Thomas, P. J. Machin, *Science* **1990**, *248*, 358–361.
[6] The first HIV protease inhibitors approved by the FDA: *Antiviral Agents Bull.* **1995**, *8*, 353–355.
[7] F. J. Palella, K. M. Delaney, A. C. Moorman, M. O. Loveless, J. Fuhrer, G. A. Satten, D. J. Aschman, S. D. Holmberg, *N. Engl. J. Med.* **1998**, *338*, 853–860.
[8] S. Grabar, C. Pradier, E. Le Corfec, R. Lancar, C. Allavena, M. Bentata, P. Berlureau, C. Dupont, P. Fabbro-Peray, I. Poizot-Martin, D. Costagliola, *AIDS* **2000**, *14*, 141–149.
[9] E. De Clercq, *J. Med. Chem.* **2005**, *48*, 1297–1313.
[10] A. Wlodawer, J. W. Erickson, *Annu. Rev. Biochem.* **1993**, *62*, 543–585.

[11] a) P. L. Darke, J. R. Huff, *Advances in Pharmacology, Vol. 25* (Eds.: J. T. August, M. W. Anders, F. Murad), Academic Press, San Diego, **1994**, pp. 399–454; b) S. Thaisrivongs, *Annu. Rep. Med. Chem.* **1994**, *29*, 133; c) M. Clare, *Drug Discovery Des.* **1993**, *1*, 49–68; d) C. Debouck, *AIDS Res. Hum. Retroviruses* **1992**, *8*, 153–164; e) J. A. Martin, *Antiviral Res.* **1992**, *17*, 265–278.

[12] a) L. Ratner, W. Haseltine, R. Patarca, K. J. Livak, B. Starcich, S. F. Josephs, E. R. Doran, J A. Rafalski, E. A. Whitehorn, K. Baumeister, L. Ivanoff, S. R. Petteway, Jr., M. L. Pearson, J. A. Lautenberger, T. S. Papas, J. Ghrayeb, N. T. Chang, R. C. Gallo, F.-W. Stall, *Nature* **1985**, *313*, 277–284; b) H. Toh, M. Ono, K. Saigo, T. Miyata, *Nature* **1985**, *315*, 691.

[13] a) L. H. Pearl, W. R. Taylor, *Nature* **1987**, *329*, 351–354; b) M. I. Johnston, H. S. Alluadeen, N. Sarver, *Trends Pharmacol. Sci.* **1989**, *10*, 305–307.

[14] a) N. E. Kohl, E. A. Emini, W. A. Schleif, L. J. Davis, J. C. Heimbach, R. A. F. Dixon, E. M. Scolnick, L. S. Sigal, *Proc. Natl. Acad. Sci. USA* **1988**, *85*, 4686–4690; b) T. J. McQuade, A. G. Tomasselli, L. Liu, B. Karacostas, B. Moss, T. K. Sawyer, R. L. Heinrikson, W. G. Tarpley, *Science* **1990**, *247*, 454–456; c) S. Seelmeier, H. Schmidt, V. Turk, K. V. Helm, *Proc. Natl. Acad. Sci. USA* **1988**, *85*, 6612–6616.

[15] For recent reviews on HIV protease inhibitors, see: a) J. P. Vacca, J. H. Condra, *Drug Discovery Today* **1997**, *2*, 261–272; b) A. Molla, G. R. Granneman, E. Sun, D. J. Kempf, *Antiviral Res.* **1998**, *39*, 1–3; c) A. Wlodawer, J. Vondrasek, *Annu. Rev. Biophys. Biomol. Struct.* **1998**, *27*, 249–284; d) A. Spaltenstein, W. M. Kazmierski, J. F. Miller V. Samano, *Curr. Top. Med. Chem.* **2005**, *5*, 1589–1607.

[16] a) J. P. Vacca, B. D. Dorsey, W. A. Schleif, R. B. Levin, S. L. McDaniel, P. L. Darke, J. Zugay, J. C. Quintero, O. M. Blahy, E. Roth, V. V. Sardana, A. J. Schlabach, P. I. Graham, J. H. Condra, L. Gotlib, M. K. Holloway, J. Lin, I. Chen, K. Vastag, D. Ostovic, P. S. Anderson, E. A. Emini, J. R. Huff, *Proc. Natl. Acad. Sci. USA* **1994**, *91*, 4096–4100; b) M. K. Holloway, J. M. Wai, T. A. Halgren, P. M. D. Fitzgerald, J. P. Vacca, B. D. Dorsey, R. B. Levin, W. J. Thompson, L. J. Chen, S. J. deSolms, N. Gafin, A. K. Ghosh, E. A. Giuliani, S. L. Graham, J. P. Guare, R. W. Hungate, T. A. Lyle, W. M. Sanders, T. J. Tucker, M. Wiggins, C. M. Wiscount, O. W. Woltersdorf, S. D. Young, P. L. Darke, J. A. Zugay, *J. Med. Chem.* **1995**, *38*, 305–317.

[17] S. W. Kaldor, V. J. Kalish, J. F. Davies, B. V. Shetty, J. E. Fritz, K. Appelt, J. A. Burgess, K. M. Campanale, N. Y. Chirgadze, D. K. Clawson, B. A. Dressman, S. D. Hatch, D. A. Khalil, M. B. Kosa, P. P. Lubbehusen, M. A. Muesing, A. K. Patick, S. H. Reich, K. S. Su, J. H. Tatlock, *J. Med. Chem.* **1997**, *40*, 3979–3985.

[18] a) D. J. Kempf, K. C. Marsh, J. F. Denissen, E. McDonald, S. Vasavanonda, C. A. Flentge, B. E. Green, L. Fino, C. H. Park, X.-P. Kong, N. E. Wideburg, A. Saldivar, L. Ruiz, W. M. Kati, H. L. Sham, T. Robins, K. D. Stewart, A. Hsu, J. J. Plattner, J. M. Leonard, D. W. Norbeck, *Proc. Natl. Acad. Sci. USA* **1995**, *92*, 2484–2488; b) D. J. Kempf, H. L. Sham, K. C. Marsh, C. A. Flentge, D. Betebenner, B. E. Green, E. McDonald, S. Vasavanonda, A. Saldivar, N. E. Wideburg, W. M. Kati, L. Ruiz, C. Zhao, L. Fino, J. Patterson, A. Molla, J. J. Plattner, D. W. Norbeck, *J. Med. Chem.* **1998**, *41*, 602–617.

[19] a) G. Bold, A. Fassler, H. Capraro, R. Cozens, T. Klimkait, J. Lazdins, J. Mestan, B. Poncioni, J. Rosel, D. Stover, M. Tintelnot-Blomley, F. Acemoglu, W. Beck, E. Boss, M. Eschbach, T. Hurlimann, E. Masso, S. Roussel, K. Ucci-Stoll, D. Wyss, M. Lang, *J. Med. Chem.* **1998**, *41*, 3387–3401; b) B. Robinson, K. Riccardi, Y.-F. Gong, Q. Guo, D. Stock, W. Blair, B. Terry, C. Deminie, F. Djang, R. Colonno, P.-F. Lin, *Antimicrob. Agents Chemother.* **2000**, *44*, 2093–2099.

[20] H. L. Sham, D. J. Kempf, A. Molla, K. C. Marsh, G. N. Kumar, C. M. Chen, W. Kati, K. Stewart, R. Lal, A. Hsu, D. Betebenner, M. Korneyeva, S. Vasavanonda, E. McDonald, A. Saldivar, N. Wideburg, X. Chen, P. Niu, C. Park, V. Jayanti, B. Grabowski, G. R. Granneman, E. Sun, A. J. Japour, D. W. Norbeck, *Antimicrob. Agents Chemother.* **1998**, *42*, 3218–3224.

[21] E. E. Kim, C. T. Baker, M. D. Dwyer, M. A. Murcko, B. G. Rao, R. D. Tung, M. A. Navia, *J. Am. Chem. Soc.* **1995**, *117*, 1181–1182.

[22] S. R. Turner, J. W. Strohbach, R. A. Tommasi, P. A. Aristoff, P. D. Johnson, H. I. Skulnick, L. A. Dolak, E. P. Seest, P. K. Tomich, M. J. Bohanon, M. M. Horng, J. C. Lynn, K. T. Chong, R. R. Hinshaw, K. D. Watenpaugh, M. N. Janakiraman, S. Thaisrivongs, *J. Med. Chem.* **1998**, *41*, 3467–3476.

[23] a) K. A. Sepkowitz, *N. Engl. J. Med.* **2001**, *344*, 1764–1772; b) T. Cihlar, N. Bischofberger, *Annu. Rep. Med. Chem.* **2000**, *35*, 177–189; c) C. W. Flexner in *Protease Inhibitors in AIDS Therapy* (Eds.: R. C. Ogden, C. W. Flexner), Marcel Dekker, New York, **2001**, pp. 139–160.

[24] a) J. A. Bartlett, R. DeMasi, J. Quinn, C, Moxham, F. Rousseau, *AIDS* **2001**, *15*, 1369–1377; b) R. M. Gulick, J. W. Mellors, D. Havlir, J. J. Eron, A. Meibohm, J. H. Condra, F. T. Valentine, D. McMahon, C. Gonzalez, L. Jonas, E. A. Emini, J. A. Chodakewitz, R. Isaacs, D. D. Richman, *Ann. Intern. Med.* **2000**, *133*, 35–39.

[25] H. Mitsuya, J. Erickson in *Textbook of AIDS Medicine* (Eds.: T. C. Merigan, J. G. Bartlet, D. Bolognesi), Williams & Wilkins, Baltimore, **1999**, pp. 751–780.

[26] a) R. M. Gulick, J. W. Mellore, D. Havlir, J. J. Eron, C. Gonzalez, D. McMahon, D. D. Richman, F. T. Valentine, L. Jonas, A. Meibohm, E. A. Emini, J. A. Chodakewitz, *N. Engl. J. Med.* **1997**, *337*, 734–739; b) S. M. Hammer, K. E. Squires, M. D. Hughes, J. M. Grimes, L. M. Demeter, J. S. Curier, J. J. Eron, Jr., J. E. Feinberg, H. H. Balfour, Jr., L. R. Deyton, J. A. Chodakewitz, M. A. Fischl for the AIDS Clinical Trials Group 320 Study Team, *N. Engl. J. Med.* **1997**, *337*, 725–733; c) S. Staszewski, J. Morales-Ramirez, K. T. Tashima, A. Rachlis, D. Skiest, J. Stanford, R. Stryker, P. Johnson, D. F. Labriola, D. Farina, D. J. Manion, N. M. Ruiz for the study 006 Team, *N. Engl. J. Med.* **1999**, *341*, 1865–1873.

[27] M. A. Wainberg, G. Friedland, *J. Am. Med. Assoc.* **1998**, *279*, 1977–1983.

[28] A. K. Ghosh, W. J. Thompson, M. K. Holloway, S. P. McKee, T. T. Duong, H. Y. Lee, P. M. Munson, A. M. Smith, J. M. Wai, P. L. Darke, J. A. Zugay, E. A. Emini, W. A. Schleif, J. R. Huff, P. S. Anderson, *J. Med. Chem.* **1993**, *36*, 2300–2310.

[29] K. Ghosh, W. J. Thompson, S. P. McKee, T. T. Duong, T. A. Lyle, J. C. Chen, P. L. Darke, J. A. Zugay, E. A. Emini, W. A Schleif, J. R. Huff, P. S. Anderson, *J. Med. Chem.* **1993**, *36*, 292–294.

[30] a) R. G. Sherrill, M. R. Hale, A. Spaltenstein, E. S. Furfine, C. W. Andrews III, G. T. Lowen, *PCT Int. Appl.* **1999**, 344 [WO 9965870]; b) M. L. Vazquez, M. L. Bryant, M. Clare, G. A. DeCrescenzo, E. M. Doherty, J. N. Freskos, D. P. Getman, K. A. Houseman, J. A. Julien, G. P. Kocan, R. A. Mueller, H. S. Shieh, W. C. Stallings, R. A. Stegeman, J. J. Talley, *J. Med. Chem.* **1995**, *38*, 581–584; c) J. A. Partaledis, K. Yamaguchi, M. Tisdale, E. D. Blair, C. Falcione, B. H. Maschera, R. E. Myers, S. Pazhanisamy, O. Futer, A. B. Cullinan, C. M. Stuver, R. A. Byrn, D. J. Livingston, *J. Virol.* **1996**, *69*, 5228–5235.

[31] a) A. K. Ghosh, W. J. Thompson, P. M. D. Fitzgerald, J. C. Culberson, M. G. Axel, S. P. McKee, J. R. Huff, P. S. Anderson, *J. Med. Chem.* **1994**, *37*, 2506–2508; b) A. K. Ghosh, J. F. Kincaid, D. E. Walters, Y. Chen, N. C. Chaudhuri, W. J. Thompson, C. Culberson, P. M. D. Fitzgerald, H. Y. Lee, S. P. McKee, P. M. Munson, T. T. Duong, P. L. Darke, J. A. Zugay, W. A. Schleif, M. G. Axel, J. Lin, J. R. Huff, *J. Med. Chem.* **1996**, *39*, 3278–3290.

[32] A. K. Ghosh, Y. Chen, *Tetrahedron Lett.* **1995**, *36*, 505–508.

[33] K. Nakanishi, *Pure Appl. Chem.* **1967**, *93*, 89–114.

[34] a) E. J. Corey, M.-C. Kang, M. C. Desai, A. K. Ghosh, I. N. Houpis, *J. Am. Chem. Soc.* **1988**, *110*, 649–651; b) E. J. Corey, A. K. Ghosh, *Tetrahedron Lett.* **1988**, *29*, 3201–3202.

[35] a) M. Uchiyama, M. Hirai, M. Nagata, R. Katoh, R. Ogawa, A. Ohta, *Tetrahedron Lett.* **2001**, *42*, 4653–4656; b) P. J. L. M. Quaedflieg, B. R. R. Kesteleyn, P. B. T. P. Wigerinck, N. M. F. Goyvaerts, R. J. Vijn, C. S. M. Liebregts, J. H. M. H. Kooistra, C. Cusan, *Org. Lett.* **2005**, *7*, 5917–5920; c) A. K. Ghosh, S. Leshchenko, M. Noetzel, *J. Org. Chem.* **2004**, *69*, 7822–7829.

[36] A. K. Ghosh, J. F. Kincaid, W. Cho, D. E. Walters, K. Krishnan, K. A. Hussain, Y. Koo, H. Cho, C. Rudall, L. Holland, J. Buthod, *Bio. Org. Med. Chem. Lett.* **1998**, *8*, 687–690.

[37] a) K. Yoshimura, R. Kato, M. F. Kavilck, A. Nguyen, V. Maroun, K. Maeda, K. A. Hussain, A. K. Ghosh, S. V. Gulnik, J. W. Erickson, H. Mistuya, *J. Virol.* **2002**, *76*, 1349–1358; b) A. K. Ghosh, E. Pretzer, H. Cho, K. A. Hussain, N. Duzgunes, *Antiviral Res.* **2002**, *54*, 29–36.

[38] a) J. W. Erickson, S. V. Gulnik, A. K. Ghosh, K. A. Hussain, *PCT Int. Appl.* **1999**, 85, pp. WO 9967254; b) S. V. Gulnik, L. J. Suvorov, B. Liu, B. Yu, B. Anderson, H. Mitsuya, J. W. Erickson, *Biochemistry* **1995**, *34*, 9282–9287.

[39] S. De Meyers, M. Peters, *Conference on retroviruses and opportunistic infections (11th CROI)*, February 8–11, **2004**, San Francisco, CA (USA), abstracts 533 and 620.

[40] Y. Koh, H. Nakata, K. Maeda, H. Ogata, G. Bilcer, T. Devasamudram, J. F. Kincaid, P. Boross, Y. F. Wang, Y. Tie, P. Volarath, L. Gaddis, R. W. Harrison, I. T. Weber, A. K. Ghosh, H. Mitsuya, *Antimicrob. Agents Chemother.* **2003**, *47*, 3123–3129.

[41] a) L. Hong, X. Zhang, J. A. Hartsuck, J. Tang, *Protein Sci.* **2000**, *9*, 1898–1904; b) G. S. Laco, C. Schalk-Hihi, J. Lubkowski, G. Morris, A. Zdanov, A.

Olson, J. H. Elder, A. Wlodawer, A. Gustchina, *Biochemistry* **1997**, *36*, 10696–10708.

[42] Y. Tie, P. I. Boross, Y. F. Wang, L. Gaddis, A. K. Hussain, S. Leshchenko, A. K. Ghosh, J. M. Louis, R. W. Harrison, I. T. Weber, *J. Mol. Biol.* **2004**, *338*, 341–352.

[43] A. Y. Kovalevsky, Y. Tie, F. Liu, P. I. Boross, Y. F. Wang, S. Leshchenko, A K. Ghosh, R. W. Harrison, I. T. Weber, *J. Med. Chem.* **2006**, *49*, 1379–1387.

[44] R. Van der Guest, I. Van der Sandt, D. Gille, K. Groen, L. Tritsmans, P. Stoffels, *Safety, Tolerability and Pharmacokinetics of Escalating Single Oral Doses of TMC114, a Novel Protease Inhibitor (PI) Highly Active Against HIV-1 Variants Resistant to Other PIs*, December, **2001**, ICAAC Meeting.

[45] On June 23, 2006, the FDA approved new HIV treatment for patients who do not respond do existing drugs. Please see: http://www.fda.gov/bbs/topics/NEWS/2006/NEW01395.html

[46] S. De Meyer, H. Azijn, D. L. N. G. Surleraux, D. Jochmans, A. Tahri, R. Pauwels, P. Wigerinck, M.-P. de Bethune, *Antimicrob. Agents Chemother.* **2005**, *49*, 2314–2321.

[47] Details of this work will be reported in due course: A. K. Ghosh et al., unpublished results.

[48] a) X. Chen, D. J. Kempf, L. Li, H. L. Sham, S. Vasavanonda, N. E. Wideburg, A. Saldivar, K. C. Marsh, E. McDonald, D. W. Norbeck, *Bioorg. Med. Chem. Lett.* **2003**, *13*, 3657–3660; b) X. Chen, L. Li, D. J. Kempf, H. Sham, N. E. Widebury, A. Saldivar, S. Vasavanonda, K. C. Marsh, E. McDonald, D. W. Norbeck, *Bioorg. Med. Chem. Lett.* **1996**, *6*, 2847–2852.

[49] a) J. F. Miller, E. S. Furfine, M. H. Hanlon, R. J. Hazen, J. A. Ray, L. Robinson, V. Samano, A. Spaltenstein, *Bioorg. Med. Chem. Lett.* **2004**, *14*, 959–963; b) J. F. Miller, M. Brieger, E. S. Furfine, R. J. Hazen, I. Kaldor, D. Reynolds, R. G. Sherrill, A. Spaltenstein, *Bioorg. Med. Chem. Lett.* **2005**, *15*, 3496–3500; c) R. G. Sherrill, E. S. Furfine, R. J. Hazen, J. F. Miller, D. J. Reynolds, D. M. Sammond, A. Spaltenstein, P. Wheelan, L. L. Wright, *Bioorg. Med. Chem. Lett.* **2005**, *15*, 3560–3564.

[50] J. F. Miller, C. W. Andrews, M. Brieger, E. S. Furfine, M. R. Hale, M. H. Hanlon, R. J. Hazen, I. Kaldor, E. W. McLean, D. Reynolds, D. M. Sammond, A. Spaltenstein, R. Tung, E. M. Turner, R. X. Xu, R. G. Sherrill, *Bioorg. Med. Chem. Lett.* **2006**, *16*, 1788–1794.

[51] D. L. N. G. Surleraux, A. Tahri, W. G. Verschueren, G. M. E. Pille, H. A. de Kock, T. H. M. Jonckers, A. Peeters, S. De Meyer, H. Azijn, R. Pauwels, M.-P. de Bethune, N. M. King, M. P. Jeyabalan, C. A. Schiffer, P. B. T. P. Wigerinck, *J. Med. Chem.* **2005**, *48*, 1813–1822.

[52] D. L. N. G. Surleraux, B. A. de Kock, W. G. Verschueren, G. M. E. Pille, L. J. R. Maes, A. Peeters, S. Vendeville, S. De Meyer, H. Azijn, R. Pauwels, M.-P. de Bethune, N. M. King, M. P. Jeyabalan, C. A. Schiffer, P. B. T. P. Wigernick, *J. Med. Chem.* **2005**, *48*, 1965–1973.

Received: April 26, 2006
Published online on August 22, 2006

JOURNAL OF VIROLOGY, Nov. 2006, p. 10683–10691 Vol. 80, No. 21
0022-538X/06/$08.00+0 doi:10.1128/JVI.01009-06

De Novo Human T-Cell Leukemia Virus Type 1 Infection of Human Lymphocytes in NOD-SCID, Common γ-Chain Knockout Mice[▽]

Paola Miyazato,[1] Jun-ichirou Yasunaga,[1] Yuko Taniguchi,[1] Yoshio Koyanagi,[2] Hiroaki Mitsuya,[3] and Masao Matsuoka[1]*

Laboratory of Virus Immunology[1] and Laboratory of Virus Pathogenesis,[2] Institute for Virus Research, Kyoto University, Kyoto 606-8507, Japan, and Department of Hematology and Department of Infectious Diseases, Graduate School of Medicine, Kumamoto University, Kumamoto 860-8556, Japan[3]

Received 17 May 2006/Accepted 21 August 2006

Human T-cell leukemia virus type 1 (HTLV-1) is the etiologic agent of adult T-cell leukemia, a disease that is triggered after a long latency period. HTLV-1 is known to spread through cell-to-cell contact. In an attempt to study the events in early stages of HTLV-1 infection, we inoculated uninfected human peripheral blood mononuclear cells and the HTLV-1-producing cell line MT-2 into NOD-SCID, common γ-chain knockout mice (human PBMC-NOG mice). HTLV-1 infection was confirmed with the detection of proviral DNA in recovered samples. Both $CD4^+$ and $CD8^+$ T cells were found to harbor the provirus, although the latter population harbored provirus to a lesser extent. Proviral loads increased with time, and inverse PCR analysis revealed the oligoclonal proliferation of infected cells. Although *tax* gene transcription was suppressed in human PBMC-NOG mice, it increased after in vitro culture. This is similar to the phenotype of HTLV-1-infected cells isolated from HTLV-1 carriers. Furthermore, the reverse transcriptase inhibitors azidothymidine and tenofovir blocked primary infection in human PBMC-NOG mice. However, when tenofovir was administered 1 week after infection, the proviral loads did not differ from those of untreated mice, indicating that after initial infection, clonal proliferation of infected cells was predominant over de novo infection of previously uninfected cells. In this study, we demonstrated that the human PBMC-NOG mouse model should be a useful tool in studying the early stages of primary HTLV-1 infection.

Human T-cell leukemia virus type 1 (HTLV-1) was the first retrovirus shown to be related to human diseases (21, 44), including adult T-cell leukemia (ATL) (50, 51, 58) and HTLV-1-associated myelopathy/tropical spastic paraparesis (HAM/TSP) (16, 43). The infectivity of free virions is much lower than that of infected cells: transmission is cell mediated (8). Glucose transporter 1 has been identified as an HTLV-1 receptor (35). After infected cells form virological synapses with uninfected cells, the viral genome is transferred into uninfected cells (23). Hence, a salient feature of HTLV-1 infection is that this virus transmits in a cell-to-cell fashion. After infection, HTLV-1 facilitates cell-to-cell transmission by forcing the proliferation of infected cells via the actions of its accessory genes.

In the early stage of HTLV-1 infection, accessory genes including *p12*, *p30*, *p13*, and *HBZ*, have been reported to be important for in vivo proliferation of infected cells (3, 5, 22, 47). The gene product p12 plays a critical role by releasing calcium from the endoplasmic reticulum to activate nuclear factor of activated T cell-mediated transcription (2). In addition, p12 enhances lymphocyte-associated antigen-1-mediated cell adhesion, which might facilitate cell-to-cell transmission of HTLV-1 (29), and downmodulates the expression of major histocompatibility complex class I antigens (26). p30 has been reported to suppress viral gene transcription by different mechanisms (41). Other functions of p30 have been also demonstrated, such as the enhancement of the transcription of cellular genes associated with cell proliferation (38, 64). In addition, the *tax* gene is believed to play a central role in proliferation of infected cells by its pleiotropic actions (14, 17, 63). On the other hand, Tax-expressing cells are rapidly eliminated in vivo, since the Tax protein is a major target antigen of cytotoxic T lymphocytes (CTLs) (4, 27). In ATL cells, Tax expression has been shown to be suppressed by several mechanisms (52), strongly suggesting that the loss of Tax expression might be advantageous at the stage of leukemia (36). These studies reveal that the host immune system plays an important role in limiting the proliferation of infected cells. During the long latency period that spans decades, this immune pressure selects those clones with enough alterations to become malignant, eventually leading to the development of ATL.

In vivo studies of HTLV-1 infection have been carried out mainly by inoculating virus-producing or HTLV-1-immortalized cell lines into different animal species (32). Rabbits proved to be an effective model for HTLV-1 infection (1, 65). In addition, monkeys and rats have been used to analyze the in vivo proliferation of HTLV-1-infected cells (7, 55). Furthermore, immunodeficient mouse strains were also able to engraft some HTLV-1-immortalized cell lines (13, 24). These animal models are useful for studying the infection or testing therapeutic agents. However, the early steps of primary HTLV-1 infection remain uninvestigated due to the lack of in vivo experiments using human lymphocytes.

The NOD-SCID (nonobese diabetic-severe combined immunodeficiency), common γ-chain knockout (NOG) mouse was shown to be an excellent recipient for transplantation of

* Corresponding author. Mailing address: Laboratory of Virus Immunology, Institute for Virus Research, Kyoto University, Shogoin Kawahara-cho 53, Sakyo-ku, Kyoto 606-8507, Japan. Phone: 81-75-751-4048. Fax: 81-75-751-4049. E-mail: mmatsuok@virus.kyoto-u.ac.jp.

▽ Published ahead of print on 30 August 2006.

human cells due to multiple immune dysfunctions (9, 25, 60). We report here the primary infection of human lymphocytes in this newly developed mouse strain and characterize the infection by measuring proviral load as well as determining the clonality pattern. Furthermore, we tested whether the existing antiretroviral drugs azidothymidine (AZT) and tenofovir blocked primary infection in this mouse model. This small animal model allows us to better understand the mechanism of HTLV-1 infection.

MATERIALS AND METHODS

Cells. Peripheral blood mononuclear cells (PBMC) were isolated from healthy blood donors by Ficoll-Paque Plus (Pharmacia, Uppsala, Sweden) density gradient centrifugation. MT-2, an HTLV-1-producing cell line (61), was used as the source of virus in all the experiments. MT-2 cells were treated with 50 μg/ml of mitomycin C (MMC) (Kyowa, Tokyo, Japan) for 30 min at 37°C in RPMI 1640 supplemented with 10% fetal bovine serum and antibiotics and washed four times with culture medium prior to inoculation into mice. PBMC of 14 healthy donors were used in the experiments. For in vitro cytotoxicity assays, PBMC were stimulated with phytohemagglutinin (PHA) (Sigma, St. Louis, Mo.) prior to use.

Mice. The NOG strain of mice, which was generated by backcross matings of C57BL/6J-γc^{null} mice and NOD/Shi-SCID mice, is homozygous for the SCID mutation and the interleukin 2Rγ allelic mutation. It was previously reported to present multiple immunological dysfunctions that include the absence of T, B, and NK cells and also impaired activity of dendritic cells (25). Mice were purchased from the Central Institute of Experimental Animals (Kanagawa, Japan) and were maintained in microisolator cages under specific-pathogen-free conditions in the animal facility of the Institute for Virus Research, Kyoto University (Kyoto, Japan). Mice were 6 to 7 weeks old at the time of the human PBMC transfer.

Transplantation of human PBMC in NOG mice and infection with HTLV-1. A total of 10^7 human PBMC were injected intraperitoneally into each mouse, producing chimeric mice, which we will refer to as hu-PBMC-NOG mice. Three days later, the mice were inoculated intraperitoneally with MMC-treated MT-2 cells (10^3 or 10^4 cells/mouse). Spleens and cells obtained from peritoneal lavage were harvested two or four weeks after injection of MT-2 cells. Human mononuclear cells were isolated by Ficoll-Paque Plus (Pharmacia) density gradient centrifugation prior to analysis. The experimental protocol was approved by the Ethics Review Committee for Animal Experimentation of Institute for Virus Research, Kyoto University. In each independent experiment, PBMC from a single donor were used.

Quantification of HTLV-1 proviral load. Genomic DNA was obtained from the samples by standard proteinase K treatment. To quantify the proviral load, we performed a real-time PCR as we described previously (62). The primers for exon 3 of the HTLV-1 *tax* gene were 5′-GAAGACTGTTTGCCCACCACC-3′ and 5′-TGAGGGTTGAGTGGAACGGA-3′, and the probe was 5′-CACCCG TCACGCTAACAGCCTGGCAA-3′. Genomic DNA (500 ng) was used for real-time PCR in a 50-μl reaction solution prepared with TaqMan Universal PCR master mix (Applied Biosystems, Foster City, CA). The amplification conditions were 50°C for 2 min, 95°C for 10 min, and then 40 cycles of 15 s at 95°C followed by 60 s at 60°C. All experiments were performed and analyzed using the ABI PRISM 7700 sequence detection system (Applied Biosystems). To measure cell equivalents in the input DNA, the recombination activating gene 1 (*RAG-1*) coding sequence in each sample was also quantified by real-time PCR. The sequences of the primers for *RAG-1* exon 2 detection were 5′-CCCACCTTGG GACTCAGTTCT-3′ and 5′-CACCCGGAACAGCTTAAATTTC-3′, and the probe was 5′-CCCCAGATGAAATTCAGCACCCACATA-3′. Amplification conditions were the same as those for *tax*. The probes were labeled with fluorescent 6-carboxyfluorescein (reporter) at the 5′ end and fluorescent 6-carboxytetramethylrhodamine (quencher) at the 3′ end. All samples were analyzed in duplicate. The DNA of freshly purified ATL cells, which harbor one copy of the HTLV-1 provirus, was used as positive control, and its proviral load was given the value of 100% when used as point of comparison.

IL-PCR. In order to study the clonality of HTLV-1 infected cells in hu-PBMC-NOG mice, we performed an inverse long PCR (IL-PCR) (10). Briefly, 1 μg of genomic DNA was first digested with EcoRI (TOYOBO, Osaka, Japan) and then self-ligated with T4 DNA ligase (TOYOBO) overnight at 4°C. Circularized DNA was then linearized with MluI (TOYOBO) to prevent amplification of the proviral sequence itself. The resulting DNA was used as template for IL-PCR, performed with LA *Taq* HS (Takara Bio Inc., Otsu, Japan). Amplification conditions were as follows: 94°C for 2 min; 40 cycles of 94°C for 30 s and 64°C for 10 min; and a final extension at 72°C for 15 min, using a Robocycler thermal cycler (Stratagene, La Jolla, CA). PCR products were electrophoresed in a 1% agarose gel and were then visualized via ethidium bromide staining.

Flow cytometric analysis. T-cell subsets of splenocytes were analyzed by flow cytometry (EPICS Coulter-Beckman, Fullerton, CA). Briefly, 10^6 cells were double stained with anti-human CD4-PC5 (Immunotech, Marseille, France) or anti-human CD8-PC5 (Immunotech) and anti-human CD45RO-fluorescein isothiocyanate (FITC) (Immunotech) or anti-human CD25-R-phycoerythrin (Caltag Laboratories, Burlingame, CA). They were also stained with anti-human CD45-FITC (Immunotech) and anti-mouse CD45-phycoerythrin (Immunotech) to assess the predominance of human cells in the recovered splenocytes. Cells were also stained with anti-human CD3-FITC (Sigma) and anti-human CD19-FITC (BD Biosciences, San Jose, CA).

Purification using magnetic beads. $CD4^+$ and $CD8^+$ T cells were isolated from 10^7 whole splenocytes by using BD IMag magnetic beads (BD Biosciences) according to the manufacturer's instructions. Positive selection of these T-cell subpopulations was performed using anti-human CD4- and anti-human CD8-conjugated magnetic particles.

Reverse transcriptase PCR (RT-PCR). RNA was extracted from splenic cells at the time of sacrifice and after 24 h of in vitro culture by using TRIzol reagent (Invitrogen, Carlsbad, CA) according to manufacturer's instructions. One microgram of total RNA was reverse transcribed by using the RNA LA PCR kit (using avian myeloblastosis virus) version 1.1 (Takara) using random primers. One microliter of cDNA was used as the PCR template. The following primers were used: 5′-CCGGCGCTGCTCTCATCCCGG-3′ and 5′-GGCCGAACATA GTCCCCCAGAG-3′ for *tax* and 5′-GCAGGGGGGAGCCAAAAGGG-3′ and 5′-TGCCAGCCCCAGCGTCAAAG-3′ for the GAPDH (glyceraldehyde-3-phosphate dehydrogenase) gene. The amplification conditions were as follows: 95°C for 2 min; 40 cycles of 95°C for 30 s, 62°C for 30 s, and 72°C for 30 s; and a final extension at 72°C for 2 min (for *tax*); 95°C for 3 min; 22 cycles of 95°C for 20 s, 57°C for 30 s, and 72°C for 1 min; and a final extension at 72°C for 7 min (for the GAPDH gene) in a thermal cycler (ASTEC, Fukuoka, Japan). PCR products were electrophoresed in a 2% agarose gel and visualized via ethidium bromide staining. For real-time PCR, an ABI PRISM 7500 sequence detector (Applied Biosystems) was used. Data were analyzed by a comparative cycle threshold method. The level of *tax* mRNA in the MT-1 cell line was used as a positive control and was assigned a value of 100 arbitrary units.

Sodium bisulfite treatment of genomic DNA. Sodium bisulfite treatment was performed as previously described (54). Briefly, 1 μg of genomic DNA was denatured in 0.3 N NaOH at 37°C for 15 min, and 1 μg of salmon sperm DNA was added to each sample to act as a carrier. Sodium bisulfite (pH 5.0) and hydroquinone were added to each sample to final concentrations of 3 M and 0.05 mM, respectively, and the reaction mixture was incubated at 55°C for 16 h. Samples were then desalted using the Wizard DNA cleanup system (Promega, Madison, WI). Finally, samples were desulfonated in 0.3 N NaOH at 37°C for 15 min.

COBRA. For a combined bisulfite restriction analysis (COBRA) (59), different regions of the HTLV-1 provirus were amplified from sodium bisulfite-treated genomic DNA (54). The nested PCRs were performed using FastStart *Taq* DNA polymerase (Roche, Mannheim, Germany) under the following conditions: 95°C for 5 min; 40 cycles of 30 s at 95°C, 30 s at each annealing temperature, and 30 s at 72°C; and 2 min at 72°C for a final extension. The sequences of the primers used, and their annealing temperatures are as described previously (54). The PCR products were digested for at least 4 h with TaqI restriction enzyme, which resulted in a single recognition site within each product. The digested PCR products were separated in a 3% Nusieve 3:1 agarose (BMA, Rockland, ME) gel. The intensity of each fragment was determined by using a densitograph (version 4.0; ATTO, Tokyo, Japan).

Treatment with reverse transcriptase inhibitors in mice. hu-PBMC-NOG mice were inoculated with 10^3 MMC-treated MT-2 cells 3 days after transfer of human PBMC and were then divided into three groups for treatment, with AZT (240 mg/kg of body weight/day) (Nacalai Tesque, Kyoto, Japan), tenofovir (130 mg/kg/day) (kindly provided by Gilead Sciences Inc., CA), or phosphate-buffered saline (PBS). They were treated immediately after MT-2 inoculation for 12 days and then sacrificed to recover spleens and cells from peritoneal lavage for analysis. Tenofovir and AZT were administered intraperitoneally 2 and 3 times a day, respectively. The control group was injected twice a day with PBS. In another experiment, two groups of mice received treatment with AZT for 7 days or tenofovir for 12 days beginning one week after infection with 10^4 or 10^3 MT-2 cells/mouse, respectively. Each independent experiment was performed using the PBMC from a single donor.

TABLE 1. Proviral load of mice inoculated with different numbers of MT-2 cells[a]

Donor	No. of MT-2 cells in inoculation	Proviral load (%)	
		Lavage specimen	Spleen
A	10^2	0.0	0.0
	10^3	0.3	0.0
	10^4	4.2	1.2
B	10^2	1.1	0.2
	10^3	2.5	0.4
	10^4	0.9	2.0
C	10^6	83.2	26.5
	10^6	97.9	71.7
	10^6	90.4	53.4

[a] Proviral loads of cells recovered from the peritoneal cavity and spleens 2 (for donors A and B) or 3 (for donor C) weeks after inoculation of the specified numbers of MT-2 cells are shown for mice initially receiving PBMC of three different human donors.

MTT assay. The inhibitory effects of tenofovir and AZT on cell growth were assessed by MTT [3-(4,5-dimethylthiazol-2-yl)-2,5-diphenyl tetrazolium bromide] assay, which is based on the reduction of MTT by metabolically active cells to a blue formazan that can be measured spectrophotometrically. PBMC of three different donors (10^5 cells/well) were cultured in the presence or absence of the RT inhibitors (serial 10-fold dilutions from 5 mM to 0.05 μM) and 20 U/ml of interleukin 2 (kindly provided by Shionogi & Co., Ltd., Osaka, Japan) in a 96-well plate for three days. Twenty microliters of MTT solution (7.5 mg/ml) was added to each well, and the plate was incubated at 37°C for 5 h. One hundred twenty microliters of the medium was removed and 100 μl of acidified isopropanol containing 4% (vol/vol) of Triton X was added to each well to dissolve the formazan crystals. Viability relative to the untreated control was determined. Drug concentrations which inhibited cell growth by 50% (i.e., 50% cytotoxic concentrations) were also calculated from these data. All assays were performed in quadruplicate.

RESULTS

De novo HTLV-1 infection of human PBMC in NOG mice. In order to establish an in vivo model for primary HTLV-1 infection of human lymphocytes, we chose NOG mice as recipients because they were proven to engraft human cells with high efficiency (25, 60). We first determined the number of MT-2 cells necessary to achieve infection in this new mouse model. We inoculated human PBMC of two different donors intraperitoneally and, three days later, injected different numbers of MMC-treated MT-2 cells, since HTLV-1 transmits efficiently only in a cell-to-cell fashion (23, 45, 61). Two weeks later, cells were recovered from the peritoneal cavity and the spleen of each mouse and proviral load was determined by real-time PCR (Table 1). A total of 10^3 MT-2 cells was enough to produce a detectable level of proviral load in both groups of NOG mice. Taking these results into account, we decided to use 10^3 or 10^4 MT-2 cells in the following experiments. Another group of mice was inoculated with 10^6 MT-2 cells and sacrificed 3 weeks later, which led to significantly increased proviral loads (Table 1).

To check the effects of different donor sources on proviral load, we inoculated PBMC from six healthy donors into NOG mice and found that the proportions of subpopulations in T and B lymphocytes did not influence proviral loads at 2 weeks after inoculation of MT-2 cells, and the proviral loads, even in mice inoculated with cells from the same donor, were variable, especially in cells from lavages (Table 2). Regarding provirus loads in spleen cells, variations were not so remarkable. In the following experiments, we used PBMC from a single donor in each experiment.

TABLE 2. Phenotypes of donor PBMC and proviral loads of cells recovered from infected hu-PBMC-NOG mice[a]

Donor	Surface markers of donor PBMC (%)[b]				Proviral load (%)[c]	
	CD3	CD4	CD8	CD19	Lavage specimen	Spleen
D	69.7	61.8	18.7	12.2	3.7	0.6
					34.0	1.4
					2.8	0.5
E	84.7	53.4	33.9	3.0	0.6	0.1
					12.6	1.0
					11.6	0.8
F	67.0	48.0	31.9	2.8	0.2	0.0
					2.7	0.2
					0.6	0.1
G	74.9	43.9	37.7	1.3	7.4	0.2
					2.8	0.6
H	80.0	62.8	18.0	1.2	2.4	0.2
					0.4	0.0
I	ND	ND	ND	ND	20.5	2.5
					0.1	0.3

[a] PBMC from the indicated donors were transferred into NOG mice, and these were sacrificed 2 weeks after inoculation of 10^4 MMC-treated MT-2 cells.
[b] The percentage of cells positive for the specified markers before transfer into mice is shown for each donor.
[c] The proviral loads of human cells recovered from peritoneal lavage and spleens of the different mice are shown as percentages, calculated as described in Materials and Methods. ND, not determined.

In order to characterize the primary infection with HTLV-1, we inoculated a group of mice with 10^4 MT-2 cells after the transfer of PBMC and analyzed them in two groups at 2 and 4 weeks postinfection (p.i.). To assess the proportions of human cells in the studied specimens, we stained recovered cells with anti-mouse-CD45 and anti-human-CD45 antibodies and analyzed them by flow cytometry. Human cells accounted for at least 85% of the recovered splenocytes two weeks after the transfer and reached more than 94% in the group analyzed at 4 weeks p.i. (data not shown). The total number of recovered human lymphocytes was much larger than the number initially inoculated. Two weeks after the transfer of 10^7 human PBMC, we were able to recover $(7.7 \pm 3.4) \times 10^7$ human cells from the spleen of MT-2-inoculated mice and $(8.1 \pm 2.7) \times 10^7$ human cells from the spleen of the control group. These results demonstrate both migration from the peritoneal cavity to the spleen and in vivo cell expansion. There was no significant difference between the numbers of recovered splenocytes from the MT-2-inoculated and the uninoculated control groups, indicating that the cell proliferation was probably due to xenogeneic stimulation. This suggests that, in the early stages, many cells are stimulated to proliferate in the NOG mouse environment regardless of HTLV-1 infection.

In order to confirm HTLV-1 infection, we amplified a frag-